

Copolymerizing Acrylonitrile and Methyl Acrylate by RAFT for Melt Processing Applications: A Synthetic Investigation of the Effects of Chain Transfer Agent, Initiator, Temperature, and Solvent

Susan A. Beck

Thesis submitted to the faculty of the Virginia Polytechnic Institute and State University in partial fulfillment of the requirements for the degree of

Master of Science

In

Macromolecular Science and Engineering

S. Richard Turner, Chair

Judy S. Riffle

Donald G. Baird

Robert B. Moore

Sue J. Mecham

March 26, 2014

Blacksburg, Virginia

Keywords: Poly(acrylonitrile-co-methyl acrylate), RAFT

Copyright 2014, Susan A. Beck

Copolymerizing Acrylonitrile and Methyl Acrylate by RAFT for Melt Processing Applications: A Synthetic Investigation of the Effects of Chain Transfer Agent, Initiator, Temperature, and Solvent

Susan A. Beck

Abstract

Statistical copolymers of acrylonitrile (AN) and methyl acrylate (MA) were successfully prepared and characterized using reversible addition-fragmentation chain transfer (RAFT) copolymerization. A typical copolymer was charged with 15 wt. % MA content. This thesis describes a systematic variation of the RAFT copolymerization variables to optimize this system. In particular, the effects of chain transfer agent, initiator, temperature, and solvent on the copolymer properties were studied.

Dedication

I dedicate this thesis to my husband, Ben Beck. You are the love of my life and without your support, this journey would have been an insurmountable challenge.

Acknowledgements

I am indebted to my advisor, James E. McGrath, for his hard work, suggestions, and encouragement. He always believed in me, and without his support, this thesis would have not been possible. This research was funded by the National Science Foundation Division of Materials Research Grant 1006630.

Table of Contents

Abstract	ii
Dedication	iii
Acknowledgements	iv
Table of Contents	v
List of Figures	vii
List of Tables	ix
Chapter I: Introduction	1
Chapter II: Literature Review	3
Acrylonitrile Copolymers and Fibers	3
Copolymerization of AN	4
Melt Processing of PAN copolymers	6
Conventional and Controlled Free Radical Polymerization	7
Controlled Radical Polymerization	9
RAFT Polymerization	10
Polymerization of acrylonitrile (AN) using RAFT	14
Thermal Characteristics of AN polymerized by RAFT	22
Conclusion of Published Synthetic Data	26
Chapter III: Experimental	27
Materials	27
Copolymerization	27
Synthetic Variables	28
Removal of RAFT End Group	28
Characterization	28
Chapter IV: Results and Discussion	32
Characterization of Copolymers by ¹ H-NMR	32
Measuring Monomer Conversion by ¹ H-NMR	33

Determination of End Groups and M_n using $^1\text{H-NMR}$	36
Investigation of Copolymerization Variables	42
Effect of Solvent	42
Effect of Concentration	45
Effect of Initiator and Temperature	46
Effect of RAFT Chain Transfer Agent	48
Qualitative Kinetic Information from $^1\text{H-NMR}$	50
Molecular weight determination	54
Measuring T_g , T_m , and T_d of RAFT PAN-co-MA materials	61
Chapter V: Conclusions	68
Chapter VI: Suggested Future Research	69
References	71

List of Figures

Figure 1. Synthesis of acrylonitrile (kPa)	3
Figure 2. Structures of comonomers	4
Figure 3. Relative reaction rates for comonomer addition. ⁶	4
Figure 4. Schematic representation of the primary reactions that occur during free-radical polymerization of acrylonitrile.	7
Figure 5. Plot of polymer molecular weight vs. monomer conversion for conventional and controlled free-radical polymerization ¹⁴	10
Figure 6. Mechanism of RAFT polymerization ³	11
Figure 7. Generic structures for commonly used RAFT agents; R group is monomer specific..	13
Figure 8. Mechanism of the pre-cross and cross termination reactions ¹⁷	14
Figure 9. Chain equilibration step of AN polymerized from PBuA macro-RAFT agent.....	17
Figure 10. In situ generation of RAFT agent from disulfide ²²	19
Figure 11. Reaction scheme for RAFT group removal with AIBN ³¹	21
Figure 12. Thermograms from DSC of PAN pellets measured in (a) argon and (b) air at 10 K/min: (1) commercial PAN sample (Aldrich), (2) PAN synthesized via the polymerization of AN in CO ₂ , and (3) PAN synthesized in DMSO in the presence of MPTC. This image was taken from Reference 25.....	23
Figure 13. Thermograms from DSC of PAN pellets measured in (a) argon and (b) air at 10 K/min: PAN was synthesized via RAFT polymerization (1-3) in the presence of (1) METC, (2) DBTC, and (3) MPTC and (4) in CO ₂ in the presence of DBTC. This image was copied from Reference 25.	25
Figure 14. Typical ¹ H-NMR spectrum of the copolymerization reaction mixture.....	33
Figure 15. Identification of the monomer peaks in a ¹ H-NMR spectrum. As the copolymerization proceeds, the methoxy functionality remains constant, while the vinyl peaks decrease. Reaction conditions: 85/15, 2165:235:3:1, CMDTC/ABCHN, 4.7M in DMSO.....	34
Figure 16 ¹ H-NMR of copolymer synthesized with CPDB at the CTA and AIBN as the initiator (Table 4, Row 1). Reaction conditions: 85/15, 2165:235:3:1, 70°C, 4.7 M in DMSO.....	38
Figure 17 ¹ H-NMR of copolymer synthesized with CPDB at the CTA and ABCHN as the initiator (Table 4, Row 2). Reaction conditions: 85/15, 2165:235:3:1, 90°C, 4.7 M in DMSO...	39
Figure 18 ¹ H-NMR of copolymer synthesized with CMDTC at the CTA and AIBN as the initiator (Table 4, Row 3). Reaction conditions: 85/15, 2165:235:3:1, 70°C, 4.7 M in DMSO...	40
Figure 19 ¹ H-NMR of copolymer synthesized with CMDTC at the CTA and ABCHN as the initiator (Table 4, Row 4). Reaction conditions: 85/15, 2165:235:3:1, 80°C, 4.7 M in DMSO...	41
Figure 20. Monomer conversion over time in EC (.) and DMSO (■). Reaction conditions: AN charged 80 wt%, 2400:3:1, CPDB/AIBN, 70°C, 7.4M.....	43
Figure 21. Anti-parallel dipolar bonding between a nitrile and ethylene carbonate.....	44
Figure 22. Monomer conversion over time in EC (♦) and DMSO (■). Reaction conditions: AN charged 85 wt%, 2400:3:1, CMDTC/AIBN, 80°C, 4.7M.....	44

Figure 23. Measured maximum monomer conversion at different monomer concentrations. TCC/AIBN/80°C in DMSO. Reactions were terminated after a maximum conversion was reached.	46
Figure 24. Expected structure of copolymer synthesized by RAFT using CPDB and CMDTC as the CTA.....	49
Figure 25. Time vs. % monomer conversion measurements for RAFT copolymers using CPDB as the CTA. Reaction conditions: 85/15, 2400:3:1, 4.7M	50
Figure 26. Time vs. % monomer conversion measurements for RAFT copolymers using CMDTC as the CTA. Reaction conditions: 85/15, 2400:3:1, 4.7 M	53
Figure 27. Example plot for intrinsic viscosity determination	55
Figure 28. Mathematical expression for molecular weights.....	55
Figure 29. (1) No chain transfer agent (2) dodecanethiol (3) CPDB. All reactions were run at 4.7M in DMSO at 80°C with AIBN as the initiator. (2) and (3) used a 2400:3:1 M:CTA:I ratio.57	57
Figure 30. Monomer conversion vs. time (♦) and M_n from universal calibration (□) from 1 to 5 hours. Reaction conditions: 85/15, 2400:3:1, CPDB/AIBN, 80°C, 4.7M	60
Figure 31. SEC light scattering traces from the data in Figure 29. The numbers above the curve represent the samples at time 1 through 5 hours.	60
Figure 32. DSC of PAN-co-MA copolymers. Reaction conditions: 2400:3:1, CPDB/AIBN, 70°C, 7.4M in EC. The M_w from LS was between 45000 and 50000 for these samples.....	62
Figure 33. Reduction of dithiobenzoate end group with Bu_3SnH	63
Figure 34. 1H -NMR of copolymer before (a) and after (b) removal of the dithiobenzoate end group.	63
Figure 35. SEC LS trace from before (1) and after (2) end group removal and molecular weight data from universal calibration and light scattering.....	64
Figure 36. DSC before (1) and after (2) end group removal. Conditions: 2 nd heat, 10°C/min, powder, exo down.	65
Figure 37. (1) 85/15, 2400:3:1, CPDB/AIBN, 80°C in DMSO at 7.4 M (2) 85/15, 2400:3:1, CMDTC/AIBN, 80°C in DMSO at 4 M	66
Figure 38. Film melt pressed at 190°C from an 82/18 PAN-co-MA.	67

List of Tables

Table 1. RAFT agents used for AN polymerization	15
Table 2. Schematic and chemical structures of polymerization components.	32
Table 3. End groups which can be derived from the CTA and initiator combination used. These end groups should account for the majority of all the end groups. The groups that could be identified by ¹ H-NMR were used to calculate a M _n value.....	36
Table 4. The denominator for Equation 4. J, K, L, M, and N refer to end groups which can be identified and integrated in 1H-NMR.	37
Table 5. AN/MA copolymer for the copolymers shown in Figures 16 through 19.....	42
Table 6. Solvent effect on AN/MA copolymer with CPDB.	43
Table 7. Solvent effect on AN/MA copolymer with CMDTC.	44
Table 8. Reported temperatures for 10 hour, 60 minute, and 10 minute t _{1/2} of AIBN and ABCHN.	47
Table 9. Experimentally measured % monomer conversion. Reaction conditions: 85/15, 2400:3:1, 4.7M.....	48
Table 10. Comparison of molecular weight data 1H-NMR, SEC, and intrinsic viscosity from Table 9, Entries 1-9.....	58

Chapter I: Introduction

Synthetic polymeric materials have had a significant impact in many aspects of our daily lives. Polyacrylonitrile (PAN) homopolymers and copolymers with 85 wt% acrylonitrile (AN) are known as acrylic fibers and were first introduced by DuPont in 1941 under the trade name Orlon™.¹ Acrylic polymers are important fiber forming materials which are used in many applications ranging from clothing, outdoor fabrics, and purification membranes. These materials are also used to make the precursor fibers for high yield carbon fiber. The worldwide market for acrylic staple fiber production was at 1.9 million tons in 2008, and in addition, acrylic production for carbon fiber has more than doubled from 30,000 tons to 61,000 tons in the past six years.² Acrylic fibers have excellent properties, however the production cost is significantly higher compared to that of other synthetic fibers, such as polyester and nylon, and this has caused a decline in the acrylic fiber market since the 1970s.¹ This cost differential is due to the requirement of producing fibers from solution processing, from which the solvent needs to be collected and recycled.

In the past 20 years, there has been a surge of work in the area of controlled free radical polymerization.³ A number of controlled free radical systems have been developed and as a result homopolymers, statistical copolymers, and block copolymers with known end groups and targeted molecular weights can all be generated under mild conditions. Despite the benefits, the slow rate of polymerization and reduced monomer conversion, compared to conventional free radical techniques, has limited the economic feasibility of these polymers.⁴

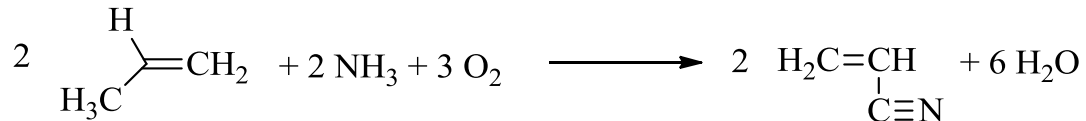
The controlled free radical technique that was employed in this work is RAFT (reversible addition-fragmentation chain transfer) polymerization. The focus of this thesis is to examine the viability of using RAFT copolymerization for producing acrylic fiber feed stocks that can be

spun by melt processing, a lower cost method than solution spinning for fiber formation. In this work, the RAFT copolymerization conditions were systematically varied to observe differences in the monomer conversion, molecular weight, comonomer content, and end groups. These differences were shown to have a marked impact on the (co)polymerization rate and monomer conversion, as well as on the degradation temperature and melting temperature. The synthetic variables examined were the RAFT chain transfer agent (CTA), initiator, solvent, concentration and temperature. The copolymers synthesized were typically charged with 85 wt. % AN (acrylonitrile), however some of the materials that will be discussed were designed to have higher or lower AN content. These materials were thoroughly characterized via different polymer characterization methods, which will be discussed further in the Experimental Section.

Chapter II: Literature Review

Acrylonitrile Copolymers and Fibers

Acrylonitrile (AN) is an important commercial monomer which is primarily synthesized via an ammoxidation called the Sohio process from propylene and ammonia⁵ (Figure 1).



- 1) Catalyst, 400-500°C, 50-200 kPa
- 2) Quench in sulfuric acid

Figure 1. Synthesis of acrylonitrile (kPa)

This monomer is a major component in synthetic rubbers like styrene-acrylonitrile copolymers and acrylonitrile-butadiene-styrene terpolymers, and is also used in acrylic, modacrylic (35-85 wt% AN), and carbon fibers. Acrylic fibers, which are classified as (co)polymers with at least 85 wt. % AN, can be made through free radical and anionic polymerization. These polymers typically have number average molecular weights (M_n) from 40-60 kg/mol and weight average molecular weights (M_w) of 90-140 kg/mol.⁶ PAN (co)polymers for acrylic fiber are synthesized using free radical polymerization, which has advantages over anionic polymerization techniques including easy introduction of cationic dye sites and reduced side reactions. Aqueous dispersion polymerization is the most popular technique for commercial production of these copolymers.⁶ Water is used as a dispersive phase and acts as a good heat sink to stabilize the exotherm of the reaction. The copolymer beads can be isolated by vacuum filtration, dried, pelletized and stored for future processing. Homogeneous free radical polymerization is also used for commercial production. A major disadvantage of this approach is that reaction times are longer due to lower

monomer and radical concentrations. Also, solvents with high chain transfer constants must be avoided for suitable molecular weights to be formed.

Copolymerization of AN

Acrylic fibers are rarely made from PAN homopolymer. The nitrile groups interact with each other causing the polymer to be rigid and difficult to dissolve. The two comonomers that are commonly incorporated with AN are methyl acrylate (MA) and vinyl acetate (VA)⁶ which are shown in Figure 2.

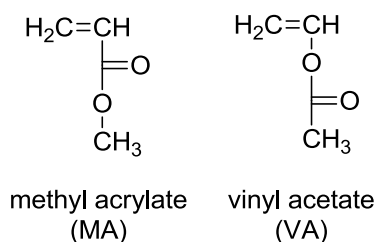


Figure 2. Structures of comonomers

These comonomers are used because they disrupt the strong polar interactions between the nitriles when statistically incorporated, improving solubility for solution processing and dyeability. The reactivity ratios, r_1 and r_2 , of a monomer pair, M_1 and M_2 , are determined by considering the rate at which a monomer reacts with the growing polymer chain, $P_n\cdot$ (Figure 3).

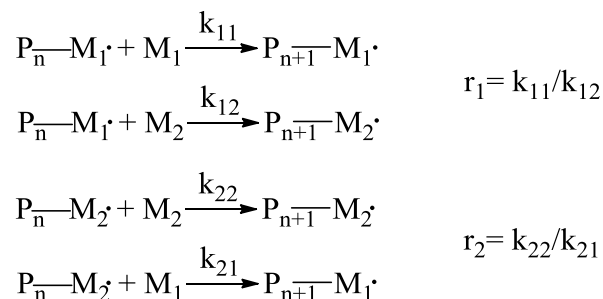


Figure 3. Relative reaction rates for comonomer addition.⁶

Statistical copolymers are formed when the reactivity ratios are both close to one. This means that neither monomer has a preference to react with itself or the other. When an r value is close

to zero, the monomer prefers to react with the comonomer. The larger the value, the more the monomer prefers to react with itself. Reported reactivity ratios for AN and MA at 68°C are $r_{AN}=1.17$ and $r_{MA}=0.76$ from in-situ FTIR⁷, indicating these monomers react in a statistical manner. AN and VA reported reactivity ratios are $r_{AN}=4.2$ and $r_{VA}=0.05$ ⁶, so in this case AN will incorporate at a much higher percentage than what is loaded. AN/VA copolymer synthesis is more effective when suspension is used because the difference in water solubility between AN and VA allows for more VA to be incorporated than the reactivity ratios would indicate. Despite the preferable reactivity of AN/MA, VA is used because of its lower cost of \$0.84/kg versus \$1.84/kg for MA.⁶

To form acrylic fibers, the PAN copolymers are dissolved into a solvent. The most commonly used solvents are dimethyl formamide (DMF), sodium thiocyanate (NaSCN), dimethylacetamide (DMAc) and nitric acid (HNO₃).⁸ The resulting dope is solution spun into fibers by extrusion through a die. The solvent is removed from the fiber through coagulation into a non-solvent, which is known as a wet spinning process, or the solvent can be removed by heating the fiber with steam, which is known as a dry spinning process. Solution spinning is costly due to solvent recycling and washing steps and is estimated to account for 44% of carbon fiber production cost.⁹ An economic and environmental alternative to solution spinning is melt spinning, which requires a stable polymer melt for about 30 minutes, from which the fibers can be directly isolated. Clearly, melt spinning PAN would lower production cost and allow the market for this material to be potentially expanded.

The current dilemma with melt spinning PAN is due to inherent degradation of the polymer prior to reaching a polymer melt stage. The degradation of PAN begins through cyclization intra- and inter-molecularly of the polar nitrile groups above 200°C which causes a

large increase in viscosity of the melt. The melting point of PAN has been measured by differential scanning calorimetry (DSC) at fast heating rates to be around 320°C.¹⁰ PAN typically is produced with atactic stereochemistry¹⁰, and likewise it has been proposed that interaction between the polar nitrile groups form a long range order as opposed to conventional crystalline domains. High polarity solvents are necessary to break up the interactions between nitrile groups so the (co)polymer will dissolve and allow it to be solution processed into fibers. An alternative approach is to incorporate an appropriate amount of comonomer to disrupt the interactions, allowing for the T_m to be reduced below the onset of degradation. Flory derived an expression which allows for the melting point to be calculated when a minor amount of comonomer is statistically incorporated into the polymer backbone (shown below).¹⁰

$$\frac{1}{T_m} - \frac{1}{T_m^\circ} = \frac{R}{\Delta H_\mu} X_B$$

T_m and T_m° are the values for the melting points of the copolymer and homopolymer, R is the gas constant, ΔH_μ is the heat of fusion per mole of crystalline repeat units, and X_B is the mole fraction of the minor comonomer.

Melt Processing of PAN copolymers

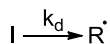
Melt processing PAN copolymers has always been of interest. Several techniques have been investigated which may be potentially viable. It is well known that water forms hydrogen bridges with the nitriles interrupting the crystallinity and significantly decreasing the melting point.¹⁰ This approach is limited because the extrusion temperature is higher than the boiling point of water, so this process needs to be pressurized through fiber formation and water removal to prevent large voids from developing during evaporation. Ongoing work is investigating different hydroxyl containing molecules such as glycerin as a higher boiling point alternative.⁹ As previously discussed, addition of a comonomer will lower the melting point.¹⁰ Standard Oil

of Ohio patented a process in 1997 for copolymerizing AN with a comonomer or comonomers (including methyl styrene, styrene, methyl methacrylate, MA, and VA) to form copolymers with up to 85 wt. % AN. It was reported that these copolymers impart melt stability over 30 minutes, an adequate melt processing window.¹¹ This concept was also shown by Bhanu et al., who reported that materials with 88:12 mol% AN:MA have stable melt viscosities over thirty minutes.¹²

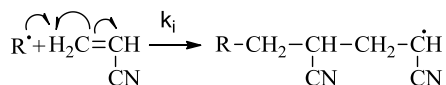
Conventional and Controlled Free Radical Polymerization

As mentioned previously, PAN copolymers for acrylic fiber applications are typically synthesized industrially using heterogeneous suspension or homogeneous solution free radical polymerization. The mechanism of a conventional free radical polymerization is illustrated in Figure 4 and involves initiation, propagation, and termination, and chain transfer steps.

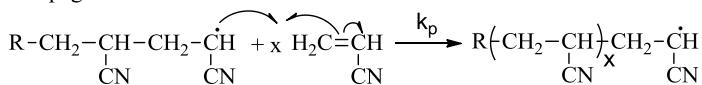
1. Formation of Radical



2. Initiation

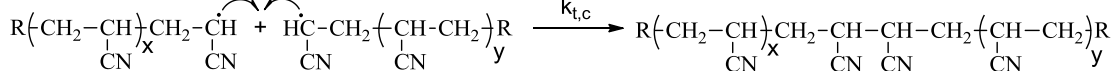


3. Propagation

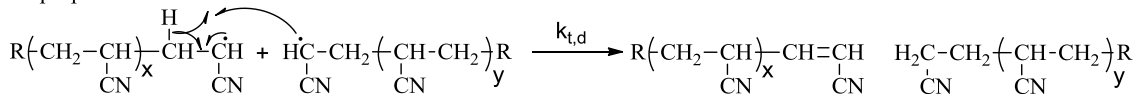


4. Termination

Combination



Disproportionation



5. Chain Transfer

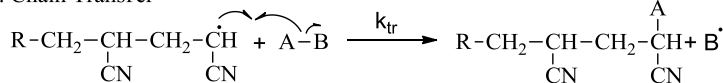


Figure 4. Schematic representation of the primary reactions that occur during free-radical polymerization of acrylonitrile.

Free radical polymerization begins with an initiator species (I) which dissociates as a result of heat or activation to produce at least one radical. The energy of this radical is high enough to break the π bond in AN, initiating a polymer chain. The radical on the end of the polymer chain continues by propagating to quickly form new bonds, leading to a high molecular weight polymer. Termination occurs when a growing polymer chain reacts with another radical species, such as another growing chain. The radicals from two active chains can combine through combination or disproportionation, which results in two dead polymer chains. Chain transfer reactions can also occur. These occur when a growing polymer chain interacts with another species to form a dead chain and radical species which may or may not be able to initiate another chain.¹³ If a high degree of chain transfer occurs which does not produce new initiator species, then inhibition of the polymerization can occur.¹³ Chain transfer can occur with other growing chains, monomer, solvent, or impurities. Chain transfer agents (CTAs) are often intentionally added to the polymerization to help reduce the molecular weight and/or add functional end groups. Each step has a unique rate constant shown in Figure 4 as k_d , k_i , k_p , $k_{t,c}$, $k_{t,d}$ and k_{tr} . The values for these rate constants are specific to the molecules involved and are also dependent on temperature and solvent. Each possible step in the mechanism will contribute to the rate of polymerization which is expressed by

$$R_p = k_p[M]^m \left(\frac{k_d f [I]}{k_{t,c}} \right)^n$$

Where [M] and [I] represent the monomer and initiator concentrations, f is the initiator efficiency, and m and n represent the rate dependence of monomer and initiator.⁶ For most polymerizations, m is 1 (1st order in [M]) and n is $\frac{1}{2}$ (half order in [I]). The majority of termination reactions occur by combination when AN is used as the monomer, so $k_{t,d}$ is not included in this expression. If chain transfer to other species is significant, k_{tr} would need to be

incorporated into this expression. It is important to note that this rate expression is most applicable to homogeneous systems, and use of a heterogeneous system can change the rate significantly.

Controlled Radical Polymerization

A true living or controlled polymerization is defined as having no termination or side reactions. The best example of this type of system is anionic polymerization. Controlled radical polymerizations can have a small amount of termination, so they are not considered truly living. However, controlled radical polymerizations do not require rigorous monomer purification like living anionic polymerization, so a large amount of work has been done in controlled polymerization because well-controlled materials can be made with less effort.

There are a handful of ways to perform controlled radical polymerization; however those which allow for the most diversity are reversible addition-fragmentation chain transfer (RAFT) polymerization and atom-transfer radical polymerization (ATRP). Each type of controlled free radical polymerization proceeds via a distinct mechanism, but the control in each comes from keeping the concentration of active radicals low. A low concentration of radicals means that termination reactions are less statistically likely. Also, the active radicals only exist for long enough to add a small amount of monomer units before returning to the dormant state. This allows for the chain growth to be more uniform leading to lower polydispersities (PDIs). The molecular weight of the chains vs. conversion is illustrated for controlled and classical free radical polymerization in Figure 5.

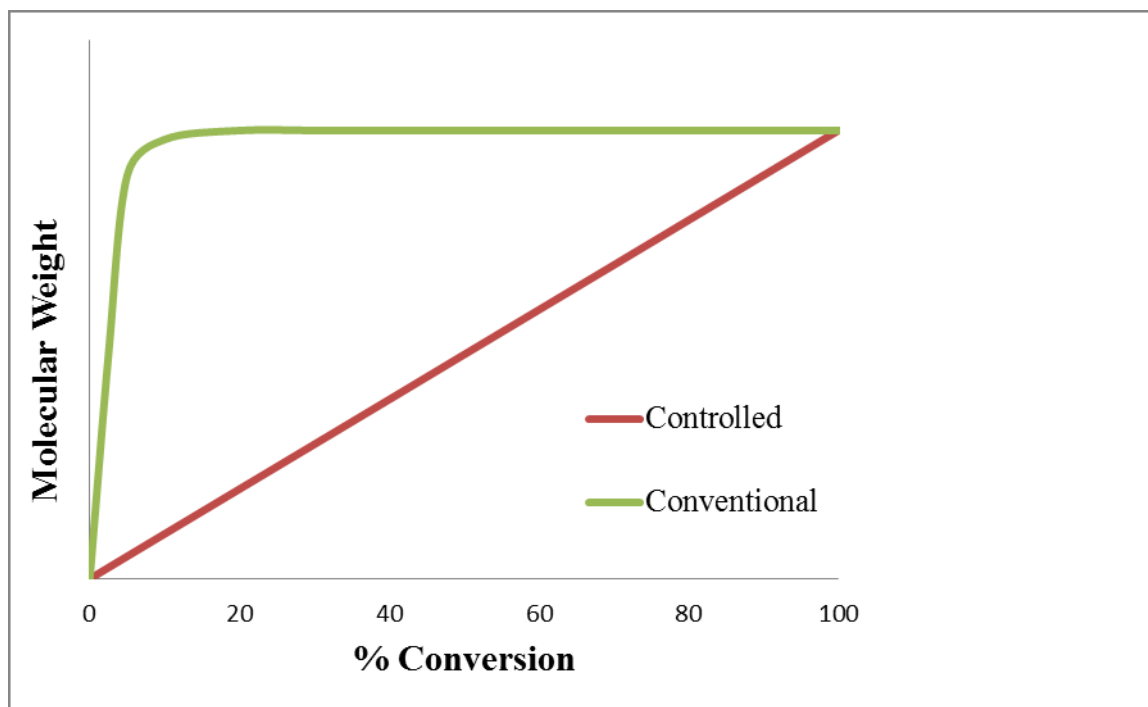


Figure 5. Plot of polymer molecular weight vs. monomer conversion for conventional and controlled free-radical polymerization¹⁴

In controlled polymerization, the low concentration of active radicals allows for uniform growth of the chains. In conventional free radical systems, there is no dormant state for the radicals so chain growth continues until a termination reaction occurs leading to a broader molecular weight distribution.

RAFT Polymerization

Although there are instances of RAFT polymerization in the patent and open literature as early as 1982, it did not become significant until 1998 when Moad, Rizzardo, Thang and colleagues published that dithiobenzoates could be used as effective RAFT chain transfer agents (CTAs).¹⁵ Since 1998, hundreds of RAFT agents have been designed and used to obtain “well-controlled” polymers. Additionally, the kinetics, mechanism, and versatility of this polymerization technique have been studied extensively.

The accepted mechanism for RAFT polymerization involves initiation, propagation, reversible chain transfer, chain equilibration, and termination steps. These steps are shown in Figure 6.

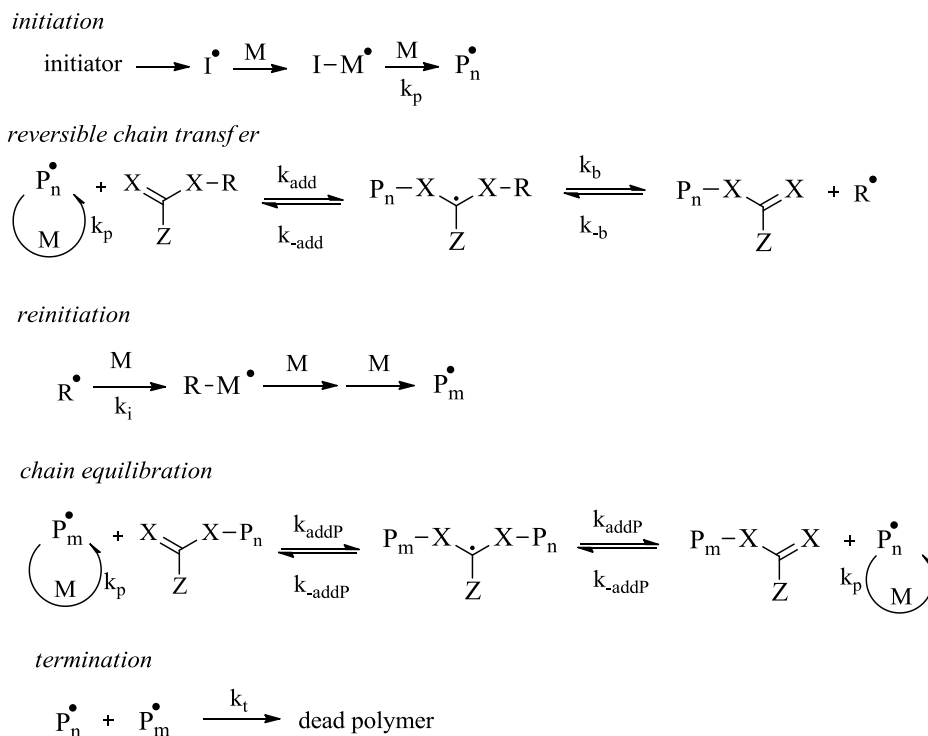


Figure 6. Mechanism of RAFT polymerization³

The initiation step for RAFT polymerization is similar to that of conventional free radical polymerization. Upon initiation, a small number of monomer units add to the chain before the growing chain (P_n^\bullet) adds to the RAFT agent at the C=S bond, forming a dormant radical species. The R group fragments from the dormant radical species forming a stable polymer-RAFT agent complex and R^\bullet initiates another polymer chain. Once the RAFT agent is consumed, an equilibrium exists between the active polymer chains adding to the stable polymer-RAFT agent and dormant polymer chains which are fragmenting. Due to the reversibility of the steps, the expression for the kinetics of this polymerization is much different than a conventional free radical system. In order to determine if a system is well controlled, the ratio of the rate constant

of reversible chain transfer (k_{tr}) and rate constant of polymerization (k_p) is compared to obtain the transfer constant (C_{tr}).³

$$C_{tr} = \frac{k_{tr}}{k_p}, \text{ where } k_{tr} = k_{add} \frac{k_{\beta}}{k_{-add} + k_{\beta}}$$

When C_{tr} is near unity, the polymerization is considered to be well-controlled because the monomer and CTA are being consumed at the same rate.

In order to minimize termination, the concentration of active polymer chains needs to be low compared to the total number of chains. The selection of R on the CTA is important because it must be able to initiate new chain growth faster than the propagation rate constant, so $k_i > k_p$. The fragmentation rate of the polymer chains must be rapid enough to prevent the dormant radical species from undergoing side reactions, such as branching or termination through combination or disproportionation with another radical species. The fragmentation rate is largely affected by substituent Z which stabilizes or destabilizes the dormant radical species.

Other factors to consider are the effect of the reaction conditions on the resulting polymer. Changes in [CTA], [M (monomer)], [I (initiator)], solvent, temperature and level of oxygen will lead to differences in the molecular weight and PDI, which in turn affect the overall polymer properties of the given materials. In RAFT polymerization, the amount of initiator is proportional to the concentration of chains without a RAFT end group in the final polymer sample. A balance between polymerization rate, desired conversion, and desired control must be established for different monomers, RAFT agents, and initiators.

The majority of RAFT CTAs are based on the thiocarbonylthio functionality. There are four distinct classes of small molecule RAFT agents as shown in Figure 7.

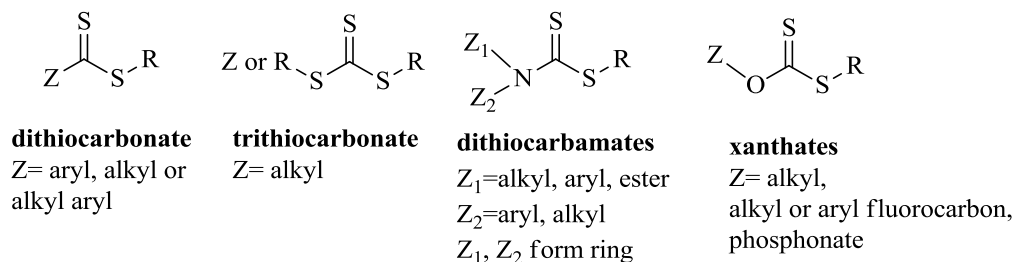


Figure 7. Generic structures for commonly used RAFT agents; R group is monomer specific

Dithiocarbamates and xanthates will not be discussed because they are more suitable for use with electron donating alkene monomers. Dithiocarbonates have a Z group that is an aryl, alkyl, or alkyl-aryl group. The R group can be any leaving group which can initiate a polymerization of a selected monomer. Dithiocarbonates have the largest k_{addP} of the classes of RAFT agents, so active chains become dormant quickly, causing monomer addition to be controlled. Likewise, these RAFT agents are well suited for monomers which have high propagation rates, such as AN and MA, because k_{tr} will be competitive with k_p , so C_{tr} will approach unity. The more well controlled the system, the higher the C_{tr} value will be.³

Retardation, meaning reduced monomer conversion over time, is a problem when a dithiocarbonate with an aromatic Z group is used because the dormant radical species is resonance stabilized. Due to resonance stabilization, pre-cross and cross termination reactions have been shown to occur between the dormant radical species and low molecular weight active radical species¹⁶ which results in cross-termination products as shown in Figure 8. In general, other issues with dithiocarbonates are hydrolytic and thermal instability.

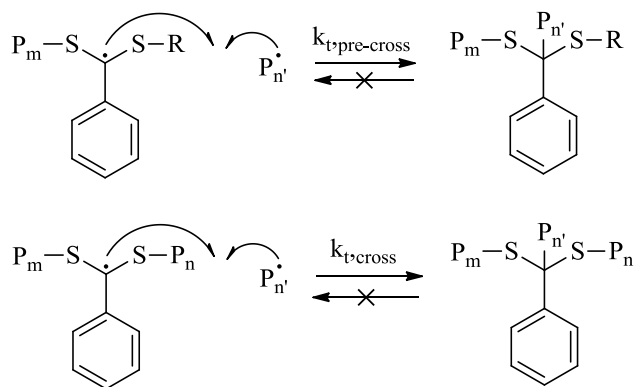


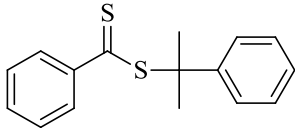
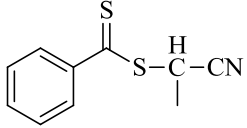
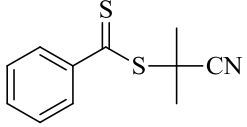
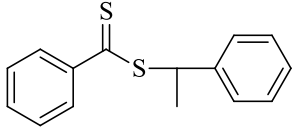
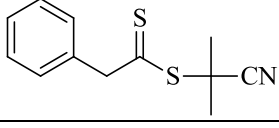
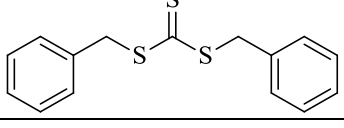
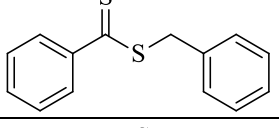
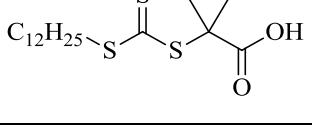
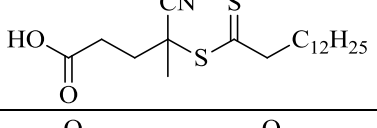
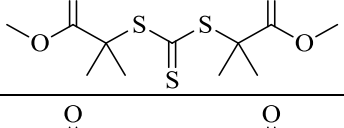
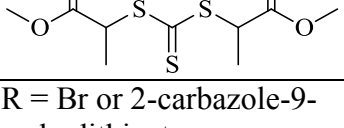
Figure 8. Mechanism of the pre-cross and cross termination reactions¹⁷

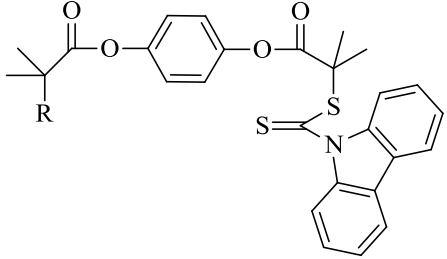
Trithiocarbonates are also used for alkene monomers with electron withdrawing groups. The $k_{P_{add}}$ is lower than with dithiocarbonates, however the polymerization of styrenic and (meth)acrylic monomers is still controlled.³ Retardation has not been observed in trithiocarbonates because the dormant radical is not as stable. This class of RAFT CTAs is more hydrolytically stable and easier to synthesize than dithiocarbonates. Accordingly, trithiocarbonates have received more attention in the recent literature.

Polymerization of acrylonitrile (AN) using RAFT

Table 1 summarizes the RAFT agents that have been used to polymerize AN. AN is a challenging monomer to polymerize because the k_p is high and the resulting PAN is insoluble in the monomer so bulk conditions cannot be used. Homogeneous polymerization of AN using RAFT has been conducted in DMF, DMSO (dimethyl sulfoxide) or EC (ethylene carbonate) to maintain polymer solubility throughout the reaction. Unless otherwise noted, AIBN (azobisisobutyronitrile) was the initiator and the freeze/pump/thaw method was used to remove oxygen from the reaction mixture.

Table 1. RAFT agents used for AN polymerization

RAFT AGENT	Name	Abbreviation	Reference(s)
	Cumyl dithiobenzoate	CDB	18 19
	2-cyano dithiobenzoate	CED	18 19
	2-cyano-2-propyl dithiobenzoate	CPBD	20 19 21 22* 23
	2-phenyl ethyl dithiobenzoate	PEDB	19 24
	2-cyano-2-propyl dithiophenylacetate	CPDA	19 22*
	Dibenzyl trithiocarbonate	DBTC	19 25 26
	Benzyl dithiobenzoate	BDTB	27
	2-dodecylthiocarbonylsulfanyl-2-methyl propionic acid	DDAT	28 29 30
	4-cyanopentanoic acid dithiobenzoate	CPADB	31
	2-methoxy-2-propyl trithiocarbonate	MPTC	25 26
	1-methoxycarbonyl ethyl trithiocarbonate	METC	25 26
R = Br or 2-carbazole-9-carbodithioate	2-bromo-2-methyl propionic acid 4-[2-	BMCCDP and	32 33

	(carbazole-9-carbodithioate)-2-methyl propionyloxy]phenyl ester AND 1,4--[2-(carbazole-9-carbodithioate)-2-methyl propionyloxy]phenyl ester	BCCDP	
* RAFT agent generated in situ			

The first publication utilizing RAFT polymerization for AN was a comparison of CDB and CED with ethylene carbonate (EC) as the solvent at 60°C.¹⁸ The polymers produced from CBD had retardation with [CBD]: [AIBN] of 10:1 (less than 5% conversion in 186 hours). When the [CDB]: [AIBN] ratio was decreased to 5:1, reasonable molecular weight polymer was obtained but PDIs reported were on the order of 2.0, so this system was not controlled. For CED, the polymerization proceeded with control even with a [CED]:[AIBN] of 10:1, as evidenced by low polydispersities. When [AN]:[AIBN]:[CED] was 2000:1:10, the polymerization reached 25.0 % in 67 hours, and when a 500:1:3 ratio was used, the conversion was 40.2 % after 7 hours. These polymers have low molecular weights (2.5 and 4.0 kg/mol as measured by ¹H-NMR end group analysis).

End group preservation with the CED polymer was tested by adding a block of n-butyl acrylate (BuA) to the PAN polymerized with CED as the RAFT agent. The block was successfully added while maintaining control of the polymerization. To test the initiation of AN from a macro-RAFT agent, BuA was polymerized using CBD. Attempts to grow AN from this macro CTA resulted in bimodal molecular weight distributions as evidenced by SEC (size

exclusion chromatography). The chain equilibrium step strongly favors PAN fragmenting, which prevents the PBuA from growing an AN block (Figure 9).

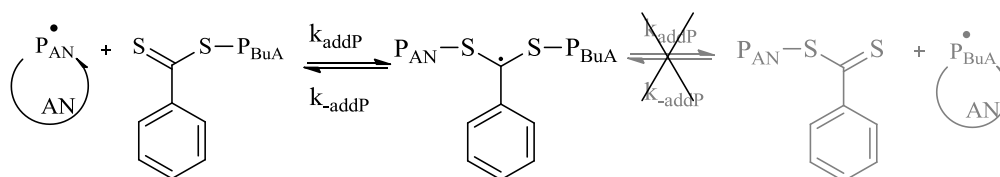


Figure 9. Chain equilibration step of AN polymerized from PBuA macro-RAFT agent

The kinetics of the RAFT polymerization of AN were studied to confirm the impact of the reaction parameters on the polymerization.²⁰ CPDB was used as the RAFT CTA and DMF was used as a solvent. The reaction variables of temperature, [M], [CTA], and [I] were explored to understand how the molecular weight, polydispersity, and retardation period varied. With increasing temperature, the retardation period was reduced due to a higher rate of consumption of the RAFT agent. When [CPDB] was increased, the retardation time was increased because CPDB had to be consumed fully before equilibrium could be reached. When [AIBN] was increased, the polymerization rate also increased.

The CED polymers¹⁸ and CPDB polymers²⁰ from the previous papers were compared with PAN made using CPDA, PEDB, CPBD, and DBTC to screen for those that would be the best CTA for AN polymerization.¹⁹ DBTC was successfully used to polymerize AN with control. This reaction was stopped at 60% monomer conversion and the polymers obtained were relatively low molecular weight (less than 9.0 kg/mol by ¹H NMR end group analysis). CDB, PEDB and CPDA did not provide control over the polymerization (polydispersities near 2.0). These CTAs have 3° and 2° benzyl radicals as the R group. The high polydispersities indicate that these 3° and 2° benzyl radicals cannot efficiently initiate AN. Combined with the high

propagation rate of AN, ineffective initiation caused the polymerization to proceed in an uncontrolled manner.

To increase the degree of polymerization, the reaction conditions were investigated using CPDB²¹, which was shown to enhance control the degree of polymerization in a previous reference.²⁰ Solvent choice was the critical aspect to high conversion in this reaction. DMF, DMSO and EC were compared at otherwise identical conditions at 60°C and 90°C, and it was found that the monomer conversion for the reactions run in EC were higher. These differences were attributed to the chain transfer ability of DMF and DMSO relative to EC. Polar interactions between the carbonyl in EC and the nitrile of AN have been reported.³⁴ This interaction may begin to explain higher monomer conversion in EC compared to DMF and DMSO, but this phenomenon needs to be studied further. The PDI of the polymers in EC was also improved compared to the other solvents, and molecular weights up to 35 kg/mol were achieved.

An et al. also explored copolymerizing AN with several different comonomers, including St, MA (methyl acrylate), MMA, BuA, and IA (itaconic acid). With 5 mol% incorporation of any one of these comonomers with AN, the overall monomer conversion was reduced. Since the AN radical propagates rapidly, addition of a slower propagating radical causes a reduction in the rate of propagation.

In the references discussed so far,^{18,19,20} the monomer conversion plateaus off before reaching high conversions. The polymerization temperature likely had an impact due to the half-life ($t_{1/2}$) of AIBN. As an example, the conversion versus time plot for the polymerizations done at 90°C leveled off at 70% conversion in three hours.²¹ Ideally, in the presence of a RAFT agent, the radical level will stay at a steady state during the polymerization to consume monomer. The $t_{1/2}$ of AIBN has been reported as 23 minutes at 90°C,³⁵ and so the majority of the initiator has

decomposed within the first hour. Without radicals being produced, termination may cause the radical concentration to decrease and the conversion to stop.

In the previous papers¹⁸⁻²¹, the RAFT agent was synthesized and added to the reaction mixture. An attempt was made to generate the RAFT agent in situ by adding in a disulfide and initiator which ideally will split into CPDB or CPDA (Figure 10).²²

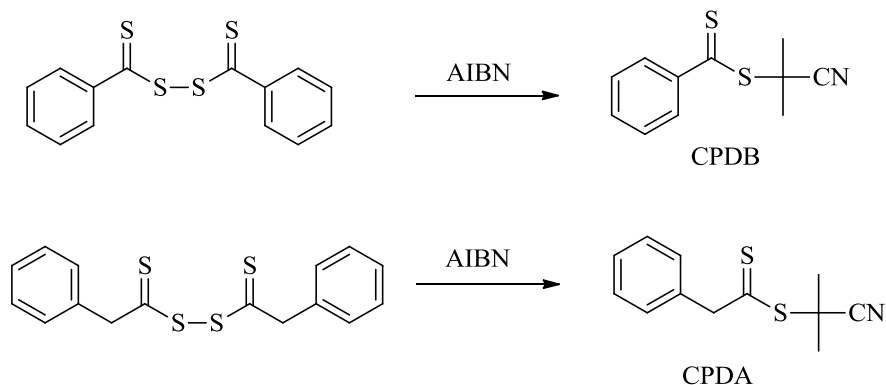


Figure 10. In situ generation of RAFT agent from disulfide²²

The materials synthesized through this method were reported to have M_n values exceeding 200 kg/mol (from SEC) and the polydispersities varied from 1.50 to 1.98. Compared to the control experiment with a polydispersity of 3.1, these reactions were somewhat better controlled, however they would not be considered well-controlled. For the CPDB disulfide, the monomer conversion was negligible unless a 1:1 ratio of CTA:AIBN was used due to retardation from this in situ approach.

There are only a few examples of AN statistical copolymerization utilizing the RAFT technique. Wan et al. copolymerized AN with HEMA (hydroxyethyl methacrylate) to form a graft copolymer. PAN-co-PHEMA was formed using BDTB as the RAFT CTA, and subsequently the HEMA was converted to an ATRP initiator to polymerize NIAM (*n*-isopropylacrylamide). Branched PAN was synthesized by Lui and coworkers by copolymerizing AN with small amount of AMA (allyl methacrylate) using CPBD.²⁷

Several articles have shown that PAN can be successfully initiated from a RAFT macro CTA. Wan et al. used a macro AN to form a block copolymer with NIAM and a comb copolymer through growing a block of HEMA then post-modifying the HEMA to an ATRP initiator. The ATRP initiator was used to form NIAM grafts.²⁸ Aquil and colleagues synthesized poly(acrylic acid)-b-PAN using DMF as the RAFT CTA.²³ Feng and colleagues attached DDAT to the surface of a CdS nanoparticle and grew PAN from the surface.²⁹ PSt was grown from PEDB then a AN oligomer (2-5 units) was grown. The PSt-b-PAN was transformed to PSt-b-poly(allyl amine) through reduction of the nitrile.²⁴ PAN-b-PDMS (poly(dimethylsiloxane)) was synthesized through modifying PDMS with DDAT at both ends.³⁰ BMCCPD (monofunctional) and BCCPD (difunctional) RAFT agents were used to polymerize high and low molecular weight PSt in the same pot. PSt was chain extended with AN, resulting in a linear increase in the degree of polymerization and a corresponding shift in the SEC data while a narrow polydispersity was maintained.³²

Only one example was found in the literature of heterogeneous suspension polymerization of AN using RAFT.³¹ PEO (polyethylene oxide) was modified with CPABD and a short block of AN was polymerized in DMF. This polymer was isolated and used as the stabilizing agent for the heterogeneous polymerization. When the RAFT agent was removed from the stabilizing polymer via reaction with AIBN (Figure 11), the suspension was unstable and the PAN aggregated and settled out of the reaction, resulting in low molecular weight materials. Keeping the RAFT agent on the polymer allowed for a stable dispersion, and PAN nanoparticles were produced. However, the PDI was 2.8, so the growth did not proceed in a controlled manner, likely due to poor transport of the RAFT agent from the water (dispersive) phase to the oil phase.

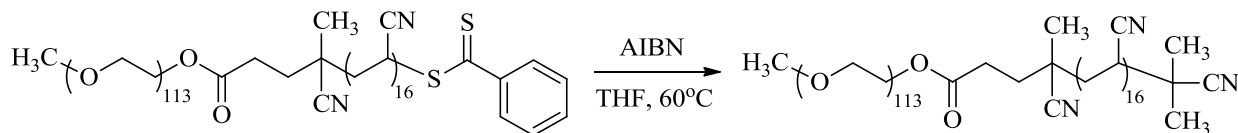


Figure 11. Reaction scheme for RAFT group removal with AIBN³¹

The most recent publication using RAFT to polymerize AN uses BCCPD and claims that a series of molecular weights ranging from 49,900 g/mol to 405,100 g/mol can be synthesized while maintaining PDIs below 1.35. These reactions were done at 75°C with a volume monomer to solvent ratio of 1:2 using AIBN as the initiator. The maximum conversion reported was 86.3% for the lowest molecular weight materials. Use of a lewis acid, AlCl₃, in the polymerization was shown to increase the isotactic fraction of the polymer from 25.4 to 33.9%.³³ The increase in isotacticity is thought to be due to the lewis acid coordinating to the nitriles on active chain end and monomer.³⁶ The coordination forces the molecules into a meso configuration and forms a bond where the nitriles are isotactic.

The kinetic differences and thermal differences between three different RAFT CTAs were explored in two recent articles.²⁵⁻²⁶ The three RAFT agents used were DBTC, MPTC, and METC. DBTC was studied by altering the reaction conditions to find the ideal temperature, CTA:AIBN ratio, and monomer:solvent ratio for AN polymerization. The polymerization was found to be more controlled at lower temperatures and lower CTA:AIBN ratios. The ratios of monomer to solvent that were examined were 1:1, 4:6, and 3:7 vol/vol AN:DMSO. For 1:1 AN:DMSO, the polymer precipitated. In 4:6 and 3:7 mixtures, the polymer remained in solution and the maximum conversion reached with DBTC was 80%. DBTC, METC, and MPTC have different reactivity as RAFT agents which correlate to the ability of the leaving group to initiate AN. AN initiated from a PAN macro RAFT agent showed a much higher activity compared to the small molecule CTAs. In this case, the AN radical was the initiator, and it could efficiently

reinitiate itself. Pressurized CO₂ was also explored as a solvent for this polymerization via RAFT and conventional free radical methods. However, since PAN is insoluble in CO₂ the polymer precipitated before a high degree of polymerization was achieved. ¹³C-NMR was conducted to determine tacticity differences between the CO₂ and solution synthesized materials. The methine carbon was assessed and the tacticity ratios were not significantly different between methods of synthesis.

Thermal Characteristics of AN polymerized by RAFT

AN polymers synthesized by RAFT were examined in argon air using DSC (Differential Scanning Calorimetry) to determine thermal characteristics.²⁵⁻²⁶ In PAN, degradation occurs through two major processes, cyclization in inert atmosphere and cyclization and oxidative degradation in air. AN synthesized with BTC as the RAFT agent was compared with a commercially available PAN purchased from Sigma-Aldrich and a PAN sample polymerized in CO₂ (without CTA) (Figure 12).

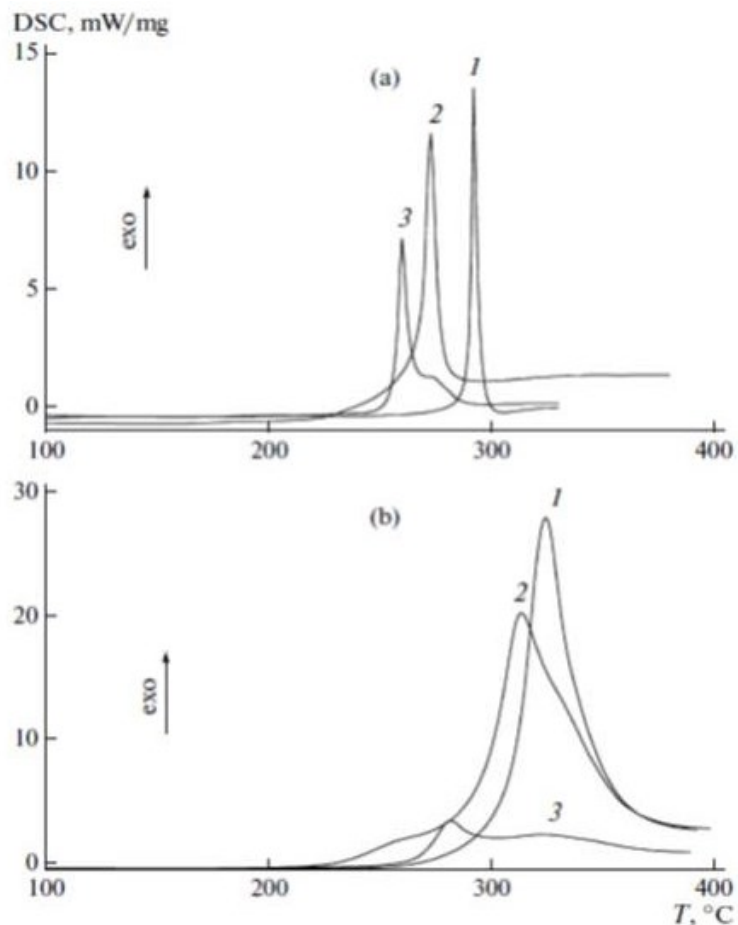


Figure 12. Thermograms from DSC of PAN pellets measured in (a) argon and (b) air at 10 K/min: (1) commercial PAN sample (Aldrich), (2) PAN synthesized via the polymerization of AN in CO₂, and (3) PAN synthesized in DMSO in the presence of MPTC. Chernikova, E. V.; Poteryaeva, Z. A.; Belyaev, S. S.; Nifant'ev, I. E.; Shlyakhtin, A. V.; Kostina, Y. V.; Cherevan, A. S.; Efimov, M. N.; Bondarenko, G. N.; Sivtsov, E. V., *Polymer Science Series B* 2011, 53 (7-8), 391-403. Used under fair use, 2014.

In the RAFT sample (Figure 12, a, (3)) the degradation began at a lower temperature and occurred over a broader temperature range with two maxima versus the commercial (Figure 12, a, (1)) and CO₂ synthesized samples (Figure 12, a, (2)) which had one maxima. In air (Figure 12, b), the exotherm was broader for all the samples and had different maxima, and the maximum exotherm occurred at higher temperature due to oxidative degradation.

The exotherm produced in the commercial (Figure 12, b, (1)) and CO₂ sample (Figure 12, b, (2)) were much higher than that of the RAFT sample. This may be due the RAFT end group degrading or leaving which may produce a radical on the polymer. This radical may kick off premature crosslinking of the PAN sample.

The degradation profiles for four RAFT polymers of similar molecular weight were compared by DSC (Figure 13).

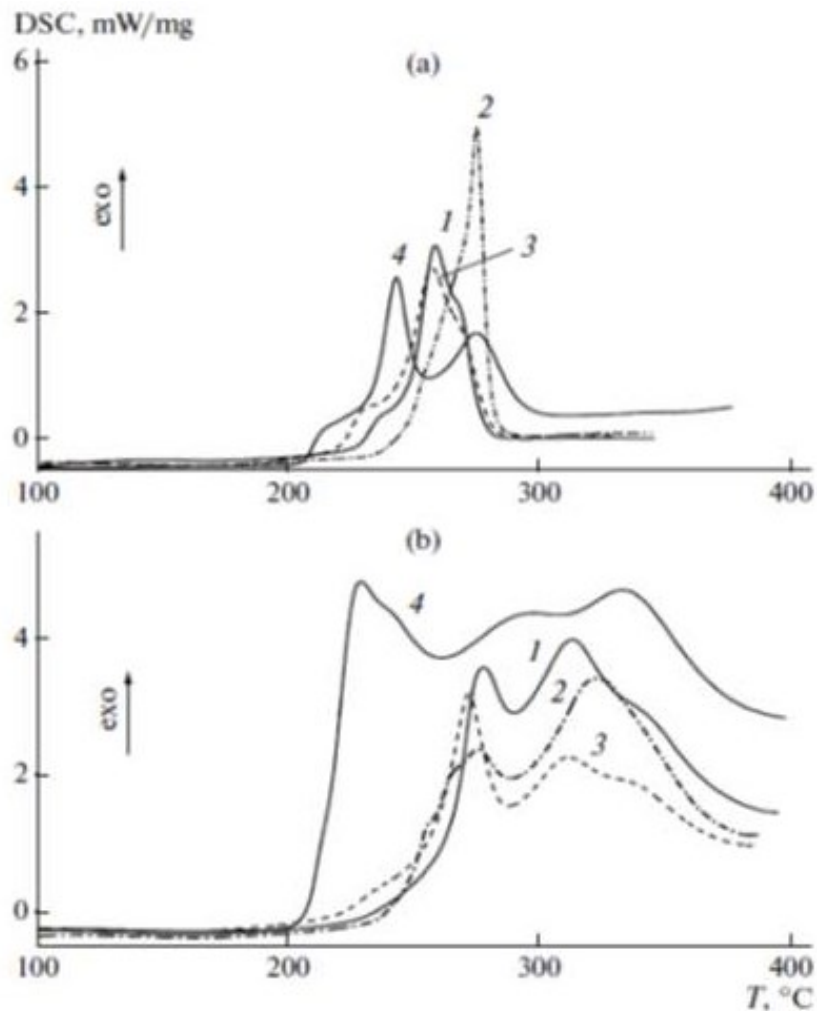


Figure 13. Thermograms from DSC of PAN pellets measured in (a) argon and (b) air at 10 K/min: PAN was synthesized via RAFT polymerization (1-3) in the presence of (1) METC, (2) DBTC, and (3) MPTC and (4) in CO₂ in the presence of DBTC. Chernikova, E. V.; Poteryaeva, Z. A.; Belyaev, S. S.; Nifant'ev, I. E.; Shlyakhtin, A. V.; Kostina, Y. V.; Cherevan, A. S.; Efimov, M. N.; Bondarenko, G. N.; Sivtsov, E. V., *Polymer Science Series B* 2011, 53 (7-8), 391-403. Used under fair use, 2014.

The DSC degradation profile was clearly dependent on the end group structure as well as the polymerization conditions. The polymers made with the METC (Figure 13, a and b, (1)) and MPTC RAFT agents (Figure 13, a and b, (3)) had similar profiles in both the argon and air tests. In argon, the BTC sample (Figure 13, a, (2)) began degrading after the other three samples.

However, in air (Figure 13, b, (2)) its degradation profile was similar to the METC (Figure 9, b, (1)) and MPTC materials (Figure 13, b, (3)). The two distinct maxima were attributed to cyclization and oxidative degradation. The CO₂ sample (Figure 13, a, (4)) differed from the other three because it had two distinct maxima, indicating two different degradation mechanisms. The CO₂ sample in air (Figure 13, b, (4)) had an exotherm that increased at 200°C sharply, which was distinctive compared to the other samples with more gradual exotherms. The degradation range was also much broader. From this data, it can be concluded that the degradation of PAN is highly dependent on the end group structure and synthetic and processing conditions.

Conclusion of Published Synthetic Data

In conclusion, the majority of the work done on RAFT polymerization of AN has been on AN homopolymers or AN block copolymers. As shown in Table 1, different RAFT agents have been used successfully to synthesize AN in a controlled manner. The reaction temperatures were 60-90°C, and the solvents used were DMF, DMSO and EC. EC appeared to provide the highest molecular weight and fastest polymerization rates, but this effect needs to be studied further. Studies involving the [CTA]:[I] ratio also indicated that the ratio of initiator to CTA cannot be too low or the polymer may not initiate and form high polymer. A majority of these studies were stopped or limited short of high conversions. Stopping controlled polymerizations at low conversions is common to preserve end group integrity and prevent termination reactions, but examples of greater than 95% conversion have been reported for MMA and VA.³⁷ There was a leveling off of the rate of polymerization reported in several of the papers, but little attempt was made to explain or overcome this problem. There are many aspects of the RAFT polymerization of AN that require further exploration.

Chapter III: Experimental

Materials

AN (99+%, Acros Organics) and MA (99%, stabilized, Acros Organics) were purified by passing through an activated alumina column (8-14 mesh, Fisher Chemical). 2-Cyano-2-propyl dithiobenzoate (CPDB, 97%, Sigma Aldrich) and cyanomethyl dodecyl trithiocarbonate (CMDTC, 98%, Sigma Aldrich) were used as chain transfer agents. 2,2'-Azobisisobutyronitrile (AIBN, 98%, Sigma Aldrich) and 1,1'-Azobis(cyclohexanecarbonitrile) (ABCHN, 98%, Sigma Aldrich) were recrystallized from methanol before use. Ethylene carbonate (EC, 99%, Sigma Aldrich) and dimethyl sulfoxide (DMSO, anhydrous, Fisher Scientific) were used as polymerization solvents as received. Methanol (Certified ACS, Fisher Scientific) and dimethyl formamide (DMF, Reagent Grade, Fisher Scientific) were used as received.

Copolymerization

The copolymers were synthesized via homogeneous RAFT polymerization. An example of an 85/15 wt% AN:MA copolymerization is as follows. AN (42.5 mL, 640.78 mmol), MA (6.3 mL, 69.70 mmol), and 100 mL DMSO were charged to an evacuated 250-mL Schlenk flask equipped with a stir bar and septa. CPDB (0.2213 g, 1.00 mmol) and AIBN (0.0547 g, 0.33 mmol) were each dissolved in 10 mL of DMSO then added to the Schlenk flask with the monomers. Oxygen was removed from the flask one of two ways. The reaction mixture was subjected to three freeze, pump, thaw cycles or sparged with N₂ for 20 minutes. The reaction mixture was then heated to 80°C in an oil bath. Monomer conversion was monitored by removing aliquots of the reaction mixture at various times and observing the ¹H-NMR spectrum to measure monomer consumption. Once the maximum monomer conversion had been achieved, propagation was stopped by removing the oil bath and adding 50 mL of DMSO to the reaction mixture. The copolymer was directly isolated by precipitation into 3L MeOH in a blender.

When EC was used as the solvent, the oxygen was removed using three freeze, pump, thaw cycles because the viscosity of the reaction mixture would not allow for a good N₂ purge. The copolymer was isolated from the reaction mixture by precipitation into 3L of DI water at 80°C in a blender. After stirring overnight, the copolymer precipitate was filtered and dissolved at 10 wt% in DMSO and reprecipitated into 3L MeOH. One additional re-precipitation was carried out in MeOH to fully remove the ethylene carbonate. All the copolymers were dried under reduced pressure at 100°C for 24 hrs. to remove any residual solvent.

Synthetic Variables

To better understand the copolymerization of AN and MA using RAFT copolymerization, several different variables were systematically altered for investigation. These variables were solvent, RAFT agent, free radical initiator, reaction temperature and concentration.

Removal of RAFT End Group

A 250-mL Schlenk flask equipped with a magnetic stir bar was charged with 15 g of PAN-co-MA (82/18 wt% AN:MA, $M_n = 47800$), AIBN (0.125 g, 0.75 mmol), Bu₃SnH (1.091 g, 3.75 mmol), and 150 mL DMSO. The freeze, pump, thaw, blanket with N₂ technique was repeated three times to remove dissolved oxygen, and the reaction mixture was heated to 80°C in an oil bath. After 3 hours, the copolymer was isolated by precipitation into 2L MeOH, filtered, then dried under reduced pressure at 100°C for 24 hours to remove any residual small molecules.³⁸

Characterization

Samples for ¹H-NMR were prepared by dissolving 20 mg copolymer in 0.7 mL DMSO-d₆ (VWR). The ¹H-NMR spectra were obtained using a Varian MR 400 MHz spectrometer with

256 scans. The AN mol% incorporation was determined by integrating the methylene region (A) (1.54-2.39 ppm), methine region (B) (3.24 – 2.57 ppm), and methoxy region (C) (3.75-3.55) (Figure 14) then using these values in Equation 1 for mol % or Equation 2 for wt. %.

$$Avg\ Mol\% AN = \frac{\left[\left(\frac{B - \frac{C}{3}}{B} + \frac{\frac{A}{2} - \frac{C}{3}}{\frac{A}{2}} \right) \right]}{\left[\left(\frac{B - \frac{C}{3}}{B} + \frac{\frac{A}{2} - \frac{C}{3}}{\frac{A}{2}} \right) + \frac{C}{3} \right]} \times 100$$

Equation 1. Determination of mol % AN incorporation into a AN-MA copolymer

$$Avg\ Wt\% AN = \frac{\left[\left(\frac{B - \frac{C}{3}}{B} + \frac{\frac{A}{2} - \frac{C}{3}}{\frac{A}{2}} \right) \times 53.06\ g/mol \right]}{\left[\left(\frac{B - \frac{C}{3}}{B} + \frac{\frac{A}{2} - \frac{C}{3}}{\frac{A}{2}} \right) \times 53.06\ g/mol \right] + \left(\frac{C}{3} \times 86.09\ g/mol \right)} \times 100$$

Equation 2. Determination of wt. % AN incorporation into an AN-MA copolymer

The number-average molecular weight ($M_{n,calc}$) of the copolymers was predicted from the monomer conversion with Equation 3.³⁹

$$M_{n,calc} = \frac{m_{AN} * ([AN]_0 - [AN]_t) + m_{MA} * ([MA]_0 - [MA]_t)}{[CTA]_0} + m_{CTA}$$

Equation 3. Determination of the theoretical M_n for AN-MA copolymers

$[AN]_0$, $[MA]_0$, $[AN]_t$, $[MA]_t$, $[CTA]_0$ correspond to the initial monomer, remaining monomer at time t, and RAFT agent concentrations. The molecular weights of the monomers and chain transfer agent are represented by m_{AN} , m_{MA} and m_{CTA} . The equation assumes that all of the end groups are from the RAFT agent and that there are two end groups per chain. A better approximation of $M_{n,calc}$ would include end groups from initiator, however information about the

initiator efficiency and initiator concentration would be required. The measured number-average molecular weight ($M_{n,NMR}$) was calculated from the total number of end groups from chain transfer agent and initiator observed in the final 1H NMR relative to the total number of repeat units as determined from Equation 4. This measurement assumes that each copolymer chain has two end groups and all of the end groups are from initiator or chain transfer agent.

$$M_{n,NMR} = \frac{\left(\frac{B - \frac{C}{3}}{B} + \frac{\frac{A}{2} - \frac{C}{3}}{\frac{A}{2}} \right) * 53.06 \text{ g/mol} + \left(\frac{C}{3} * 86.09 \text{ g/mol} \right)}{\frac{\text{Integral value from CTA}}{\# \text{ of Protons}} + \left[\frac{\text{Integral value from I}}{\# \text{ of Protons}} \right] / 2}$$

Equation 4. Determination of $M_{n,NMR}$ for AN-MA copolymers

The intrinsic viscosity ($[\eta]$) was extrapolated from the reduced and inherent viscosities of 1.0, 0.66, 0.5, and 0.4 g/dL copolymer solutions in DMF at 25°C using a Cannon Ubbelohde viscometer (100, F517). The M_v (viscosity molecular weight) was calculated from the $[\eta]$ using the Mark-Houwink-Sakurada equation using a K value of 0.000213 dL/g and an a value of 0.743. The K and a value were determined from a 91.5/8.5 w/w statistical poly(acrylonitrile-methyl acrylate) copolymer,⁴⁰ and therefore, the M_v values reported for these data are approximate. Absolute weight-average molecular weights (M_w) and molecular weight distributions (M_w/M_n) of the copolymers were determined with an Agilent 1260 infinity multi-detector SEC equipped with a Wyatt Heleos II 18 angle SLS detector, a Wyatt Viscostar viscosity detector, and a Wyatt T-rex differential RI detector at 50°C using three PLgel 10 micrometer mixed-B 200 x 75 mm columns in series. N,N-dimethyl pyrrolidone containing 0.05M LiBr was used as the mobile phase.

The glass transition temperature (T_g), melting temperature (T_m) and degradation temperature (T_d) values were obtained using Differential Scanning Calorimetry (DSC)

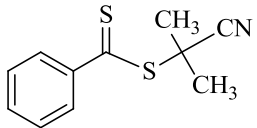
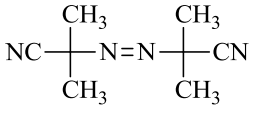
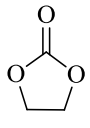
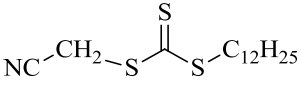
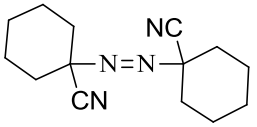
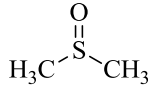
thermograms measured on a Thermal Analysis Q1000 instrument at 10°C/min using a heat (-20 to 150°C) /cool (150 to -20°C)/ heat (-20 to 300°C) cycle program.

To illustrate melt processability, approximately 2 grams of 82/18 wt% PAN-co-MA were placed between two steel plates and melt pressed into a 4"x 4" film at 190°C and 5000 psi using a Carver hydraulic unit model 3912 press.

Chapter IV: Results and Discussion

The primary thrust of this thesis was to alter the variables of the copolymerization of AN and MA using the RAFT polymerization method to increase the monomer conversion. The reaction scheme for the copolymerization via RAFT and the variables investigated are shown in Table 2.

Table 2. Schematic and chemical structures of polymerization components.

$\begin{array}{c} \text{H}_2\text{C}=\text{CH} \\ \\ \text{C}\equiv\text{N} \end{array} + \begin{array}{c} \text{H}_2\text{C}=\text{CH} \\ \\ \text{C}=\text{O} \\ \\ \text{O}-\text{CH}_3 \end{array} \xrightarrow[\text{Free Radical Initiator}]{\text{RAFT CTA}} \left[\left(\text{CH}_2-\underset{\text{CN}}{\text{CH}} \right)_x \left(\text{CH}_2-\underset{\text{C}=\text{O}}{\text{CH}} \right)_{1-x} \right]_{\text{Solvent}} \left[\begin{array}{c} \text{O} \\ \\ \text{O}-\text{CH}_3 \end{array} \right]$		
RAFT CTA	Free Radical Initiator	Solvent
Cyanopropyl dithiobenzoate 	2,2'-azobis(isobutyronitrile) 	Ethylene Carbonate 
Methyl cyano trithiocarbonate 	2,2'-azobis(cyclohexylnitrile) 	Dimethylsulfoxide 

In addition to the RAFT CTA, solvent, and free radical initiator, the temperature of the reaction and monomer concentration were also varied. Before discussing these variables, it is important to be able to interpret the differences between the copolymers so $^1\text{H-NMR}$ characterization of these materials will be discussed first.

Characterization of Copolymers by $^1\text{H-NMR}$

$^1\text{H-NMR}$ is an important characterization technique in polymer synthesis which provides valuable information about the % monomer conversion, copolymer composition, end group

concentrations, tacticity, purity, and kinetic information. In this work, the reaction conditions were varied and $^1\text{H-NMR}$ was the primary technique used to determine if there was an improvement in the monomer conversion rate and maximum extent of conversion. The $^1\text{H-NMR}$ spectra taken during the copolymerization were used to determine % monomer conversion and qualitative kinetic information, and the spectra taken of the final purified product was used to determine copolymer composition, end group concentration, and a measured number average molecular weight ($M_{n,\text{NMR}}$).

Measuring Monomer Conversion by $^1\text{H-NMR}$

The monomer conversion was measured by the change in monomer concentration versus that of the initial monomer concentration. Figure 14 shows a typical $^1\text{H-NMR}$ spectrum of an aliquot that was taken from the reaction mixture which contains AN and MA monomers and poly(acrylonitrile-co-methyl acrylate).

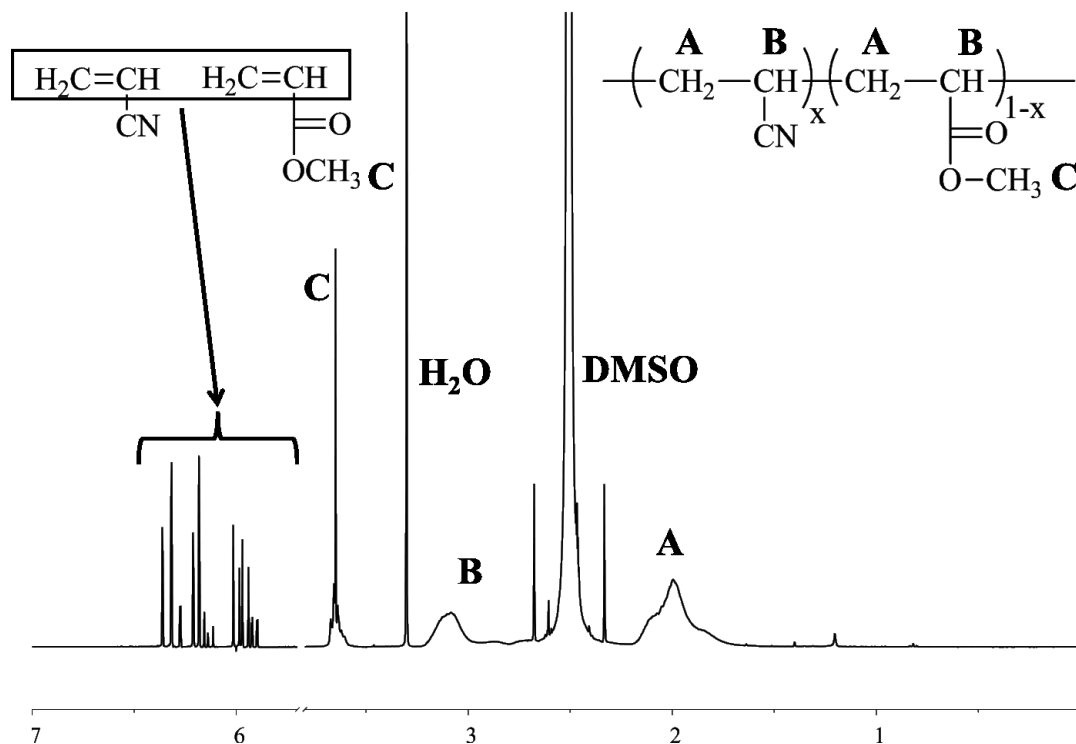


Figure 14. Typical $^1\text{H-NMR}$ spectrum of the copolymerization reaction mixture.

The vinyl protons of the monomers were in the 5.8-6.4 ppm range, which are further downfield than the protons in the copolymer backbone which are labeled A and B. The methoxy proton provided a reference point to measure monomer conversion because these protons do not significantly change position between the monomer and copolymer. Figure 15 identifies the individual peaks from each of the vinyl protons as well as shows the progression of the copolymerization over time.

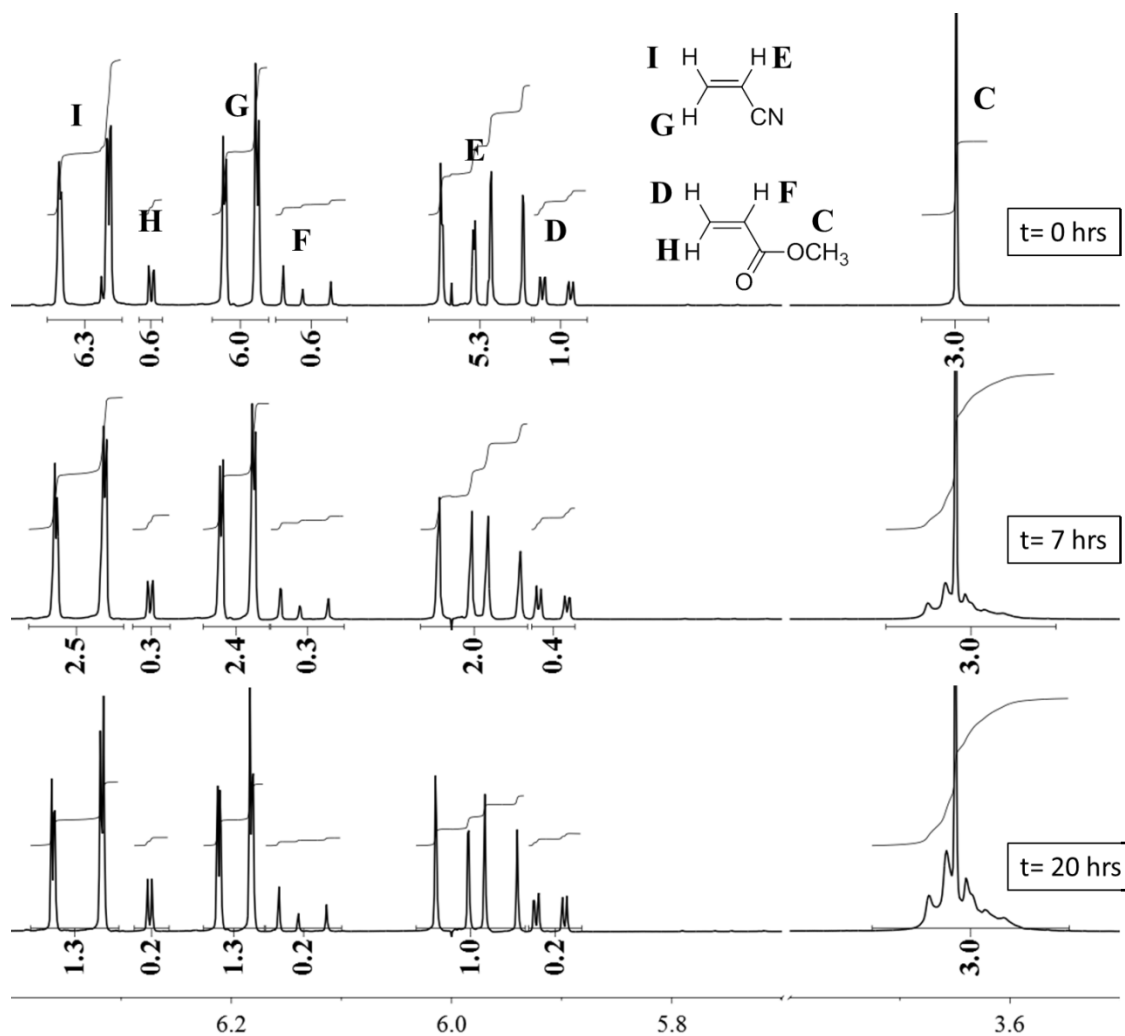


Figure 15. Identification of the monomer peaks in a $^1\text{H-NMR}$ spectrum. As the copolymerization proceeds, the methoxy functionality remains constant, while the vinyl peaks decrease. Reaction conditions: 85/15, 2165:235:3:1, CMDTC/ABCHN, 4.7M in DMSO

The peaks from the vinyl groups were split into doublets of doublets because each proton sees two unique protons. As the reaction proceeded, the integration value of the vinyl groups decreased, indicating that the monomer was being incorporated into the copolymer. The % monomer conversion is a straightforward calculation which assumes the methoxy integration remains constant throughout the copolymerization (Equation 5).

$$\% \text{ Monomer Conversion at } t = y = \left(\frac{(\sum D \text{ thru } I \text{ at } t = 0 - \sum D \text{ thru } I \text{ at } t = y)}{\sum D \text{ thru } I \text{ at } t = 0} \right) * 100$$

Equation 5. Determination of monomer conversion at time y. Peaks D thru I are shown in Figure 15

In Figure 15, the monomer integration decreased by about 40%, from 0 to 7 hours, and another 20% from 7 to 20 hours. for both the AN and MA peaks. This confirms qualitatively that the copolymer was formed statistically.

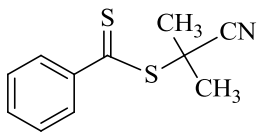
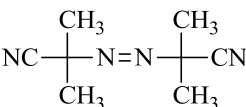
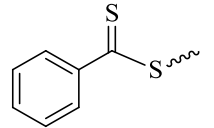
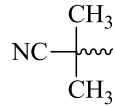
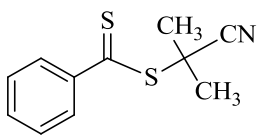
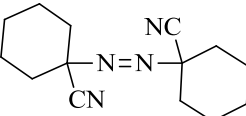
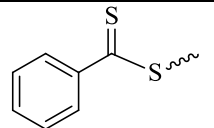
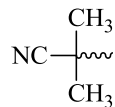
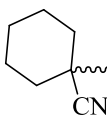
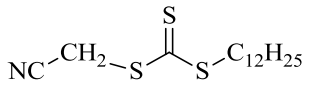
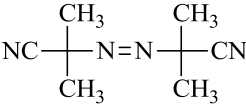
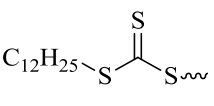
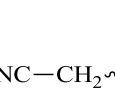
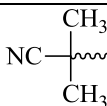
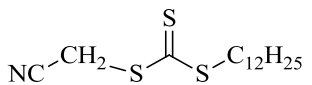
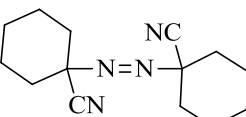
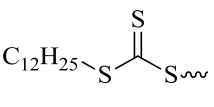
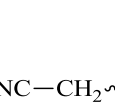
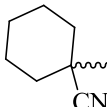
The methoxy group peak (Figure 15, peak C) broadens over the course of the reaction which suggests incorporation into the copolymer backbone because molecular motion is reduced. A second peak begins to emerge slightly further downfield (3.658 ppm) indicating that these protons became more deshielded. This was likely due to the methyl acrylate moiety being physically surrounded by nitrile groups.⁴¹

For most of the copolymerization reactions, several samples were taken throughout the course of the reaction to determine the reaction progression. These measurements provided qualitative information to determine if the copolymerization is well-controlled and will be discussed later. The final conversion was measured by taking a sample directly prior to stopping the copolymerization.

Determination of End Groups and M_n using $^1\text{H-NMR}$

As shown in Table 2, there were two CTAs and two initiators investigated in this work. Based on the proposed mechanism of RAFT polymerization, the possible end groups for each of these CTA and initiator combinations were determined, and are shown in Table 3.

Table 3. End groups which can be derived from the CTA and initiator combination used. These end groups should account for the majority of all the end groups. The groups that could be identified by $^1\text{H-NMR}$ were used to calculate a M_n value.

	CTA	Initiator	Possible End groups from CTA and initiator		
1			 J, K, L	 M	
2			 J, K, L	 M	
3			 N, O	 M	
4			 N, O	 M	

The bold letters under the end groups represent $^1\text{H-NMR}$ spectra identification (Figures 16 thru 19). For each CTA/initiator combination, the majority of the end groups should come from the

CTA and there should also be some from the initiator. For each sample, the polymer backbone protons (Figure 14, peaks A, B, C) and end group protons were identified in the $^1\text{H-NMR}$, and the integration values were used to determine $M_{n,NMR}$ using Equation 4 (pg. 30). In the four different cases shown in Table 3, the denominator of Equation 4 will depend on the specific end groups. Table 4 shows how the denominator for each of these cases.

Table 4. The denominator for Equation 4. J, K, L, M, and N refer to end groups which can be identified and integrated in $^1\text{H-NMR}$.

Entry from Table 3	$\frac{\text{Integral value from CTA}}{\# \text{ of Protons}} + [(\frac{\text{Integral value from I}}{\# \text{ of Protons}})/2]$
1	$\frac{J + K + L}{5} + \frac{(\frac{M - 6}{6})}{2}$
2	$\frac{J + K + L}{5} + \frac{(\frac{M}{6})}{2}$
3	$\frac{N}{3} + \frac{(\frac{M}{6})}{2}$
4	$\frac{N}{3}$

In Figure 16, a representative copolymer spectrum is shown of a polymer where CPDB and AIBN were used as CTA and initiator.

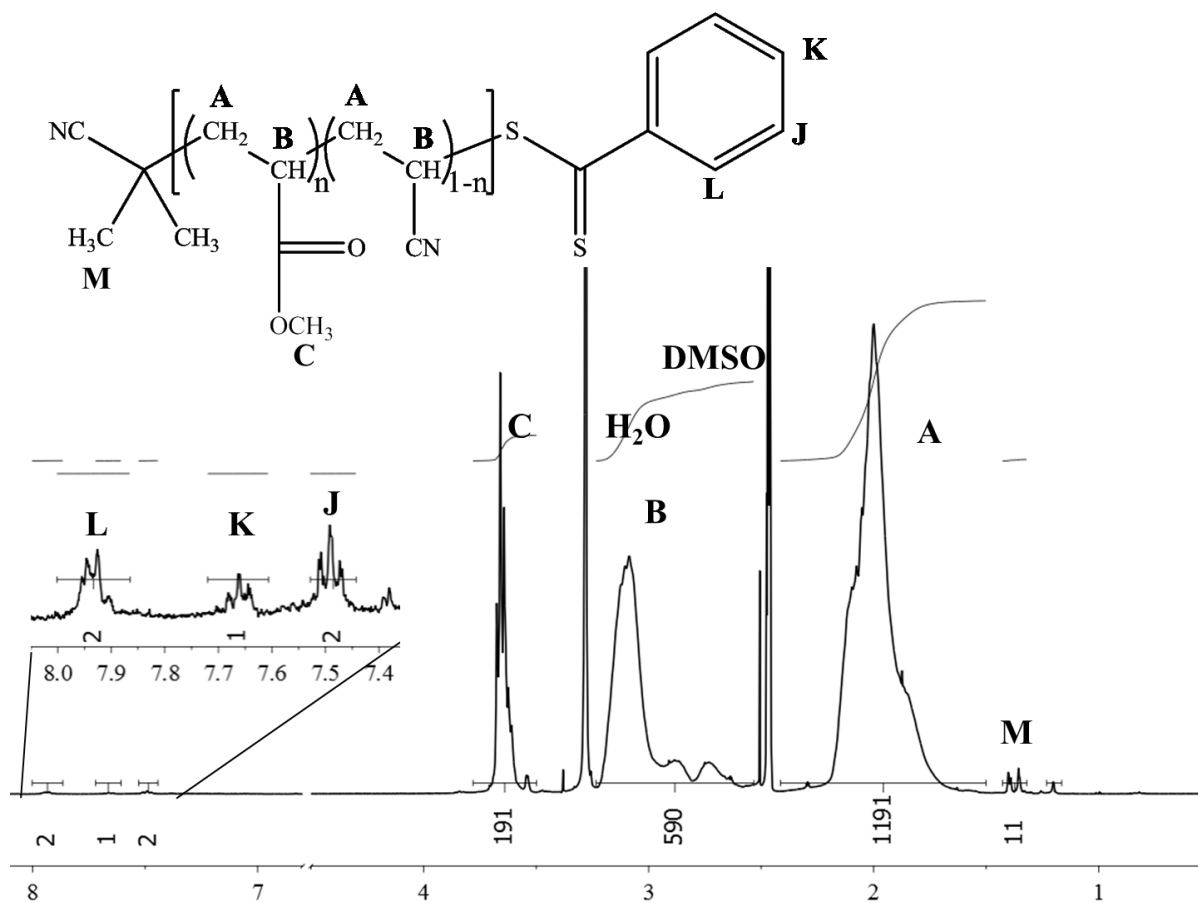


Figure 16 $^1\text{H-NMR}$ of copolymer synthesized with CPDB at the CTA and AIBN as the initiator (Table 4, Row 1). Reaction conditions: 85/15, 2165:235:3:1, 70°C, 4.7 M in DMSO

The aromatic protons (J, K, L) of CPDB are clearly identified from 7.4 to 8 ppm, and were integrated and applied as one end group. The cyanopropyl group (M) accounted for the other side of CPDB and counts for six protons based on the aromatic integration. Since M was also formed from the decomposition of AIBN, the amount of end groups from initiator were determined by subtracting six from the total integration value of the doublet at 1.38 ppm. For the example in Figure 16, the end group from initiator value was five.

Figure 17 was a typical spectrum for a polymer synthesized using CPDB and ABCHN as the CTA and initiator.

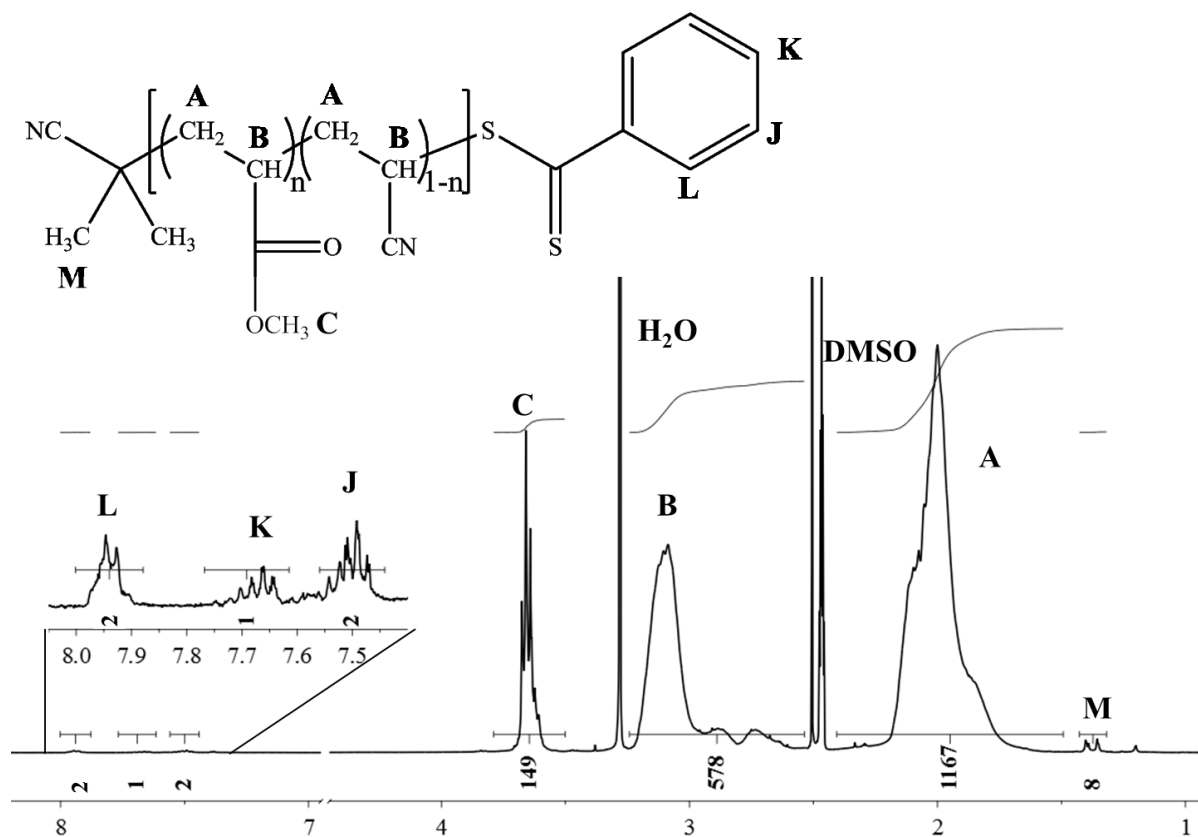


Figure 17 $^1\text{H-NMR}$ of copolymer synthesized with CPDB at the CTA and ABCHN as the initiator (Table 4, Row 2). Reaction conditions: 85/15, 2165:235:3:1, 90°C, 4.7 M in DMSO

This spectrum was visually similar to Figure 16. As indicated in

Table 3, there should be cyclohexanecarbonitrile end groups from the initiator, ABCHN. Using the $^1\text{H-NMR}$ of the initiator as a reference, it was expected that these protons would be in the region from 0.5 to 1.6 ppm. Close inspection of this area does not reveal any additional peaks which may be from this end group, so it was assumed that it was incorporated at a low level and was excluded from the $M_{n,\text{NMR}}$ calculation.

Figure 18 and Figure 19 show typical spectra for polymers synthesized using CMDTC as the CTA and AIBN and ABCHN as the initiators, respectively.

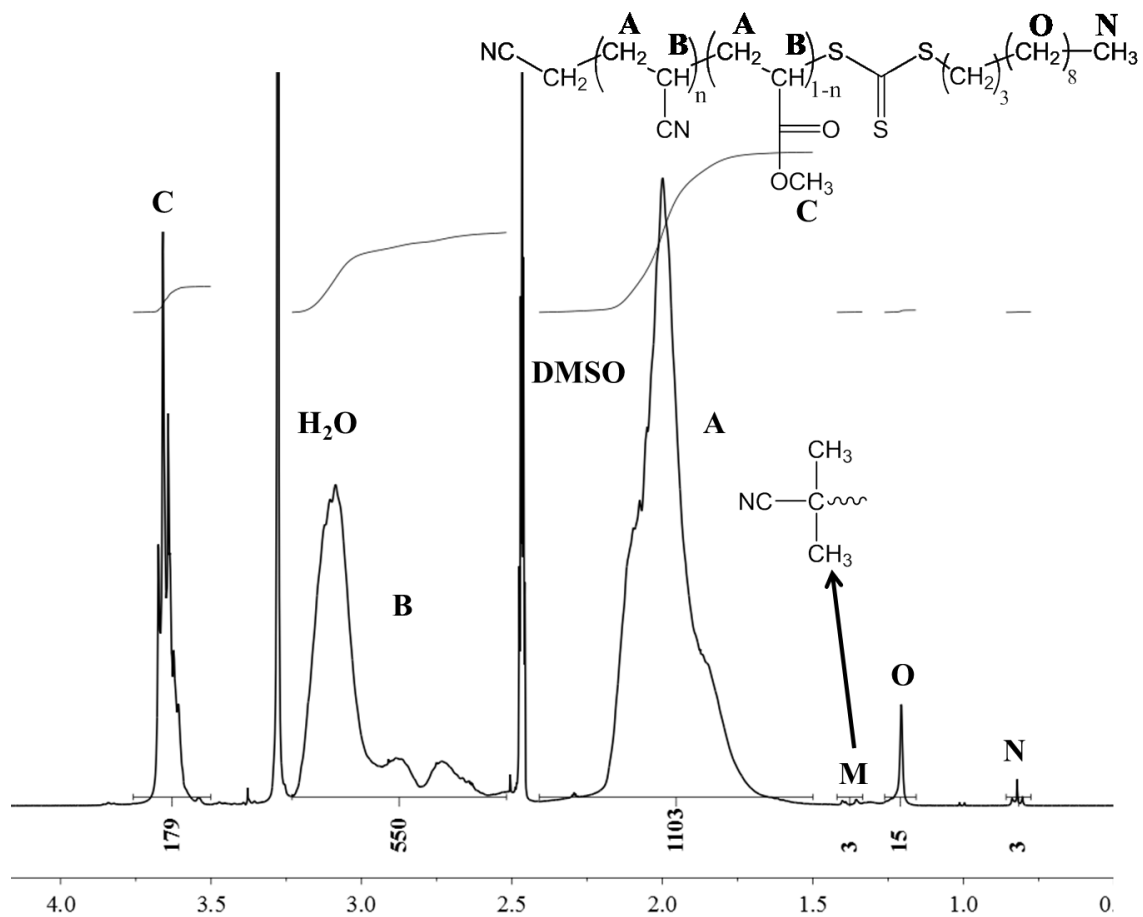


Figure 18 ¹H-NMR of copolymer synthesized with CMDTC at the CTA and AIBN as the initiator (Table 4, Row 3). Reaction conditions: 85/15, 2165:235:3:1, 70°C, 4.7 M in DMSO

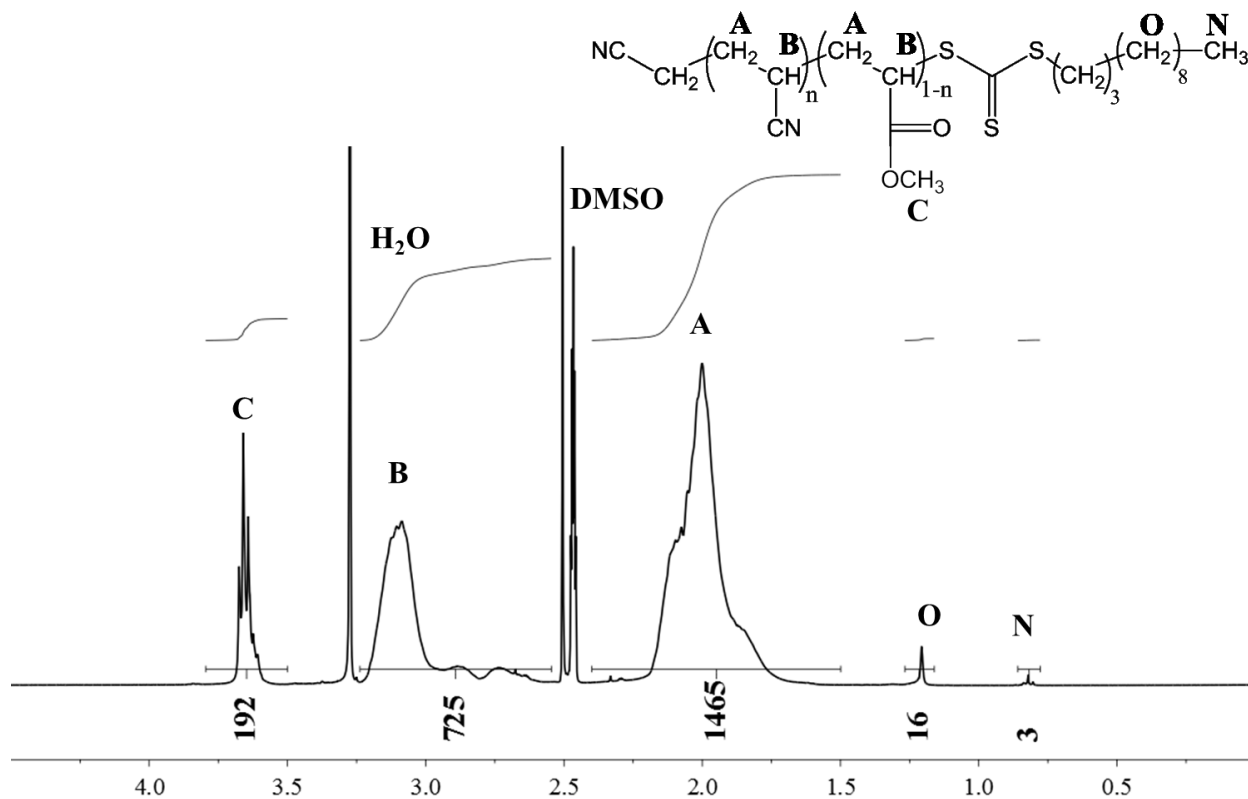


Figure 19 ¹H-NMR of copolymer synthesized with CMDTC at the CTA and ABCHN as the initiator (Table 4, Row 4). Reaction conditions: 85/15, 2165:235:3:1, 80°C, 4.7 M in DMSO

In Figure 18, N was identified as the terminal methyl on the dodecyl of CMDTC (3 protons), and O was identified as the internal protons of the dodecyl. The protons from AIBN were identified as M. The R group for CMDTC is a cyanomethyl, and these protons are shifted downfield and hidden underneath the copolymer backbone methine protons because they are directly beside an electron-withdrawing group. Figure 19 was similar to Figure 18, except the peaks at 1.4 from AIBN were not present. As in Figure 17, where ABCHN was also used as the initiator, there were no visible peaks in Figure 19 which were due to a cyclohexanenitrile end group.

For each of these spectra, the integral values are shown on the x axis. Table 5 shows the values calculated for AN incorporation, % conversion, $M_{n,calc}$ and $M_{n,NMR}$.

Table 5. AN/MA copolymer for the copolymers shown in Figures 16 through 19.

Figure	CTA/ Initiator	T (°C)	AN charged (wt %)	AN measured (wt %) ^a	% conv ^b	M _{n, calc} (g/mol) ^c	M _{n, NMR} (g/mol) ^d
16	CPDB/AIBN	70	85	85	55	22,200	23,800
17	CPDB/ABCHN	90	85	88	49	19,900	32,600
18 ^e	CMDTC/AIBN	70	85	86	79	31,800	25,800
19	CMDTC/ABCHN	80	85	88	74	29,600	41,000

^aEquation 2

^bEquation 5

^cEquation 3

^dEquation 4

^eIn this example, the M_{n,calc} is greater than M_{n,NMR}. This is not the typically observed trend for the copolymerization of AN and MA. A smaller M_{n,NMR} indicates that there were more end groups present than accounted for in the M_{n,calc}.

The AN incorporated into the copolymer was typically slightly higher than the charged value, most likely because AN has a slightly higher reactivity with itself versus MA. M_{n,calc} and M_{n,NMR} values do not agree well, except in the first case. The disagreement between the calculated and measured M_n's may be due to several factors, including combination termination reactions and not all of the end groups being accounted for. The M_{n,NMR} values are sensitive to the area of the integral which also causes some error.

As shown in this section, ¹H-NMR spectra provide information about the copolymer composition, % monomer conversion, and end group concentration. This information can be used to help determine the effect of changing reaction variables.

Investigation of Copolymerization Variables

Effect of Solvent

The polymerization solvents used in this work were EC and DMSO, which are known to solubilize AN copolymers, are relatively non-toxic, and have low chain transfer constants. Table

6 shows data for copolymerization using CPDB and AIBN for reactions where only the solvent was varied.

Table 6. Solvent effect on AN/MA copolymer with CPDB.

Solvent	CTA/I	Temp	% Conv	$M_{n, calc}$	$M_{n, NMR}$
EC	CPDB/AIBN	70	70	28,200	32,000
DMSO	CPDB/AIBN	70	55	22,200	24,000

The monomer conversion is significantly lower in DMSO when this CTA and initiator combination is used. The monomer conversion was measured over time and is shown in Figure 20.

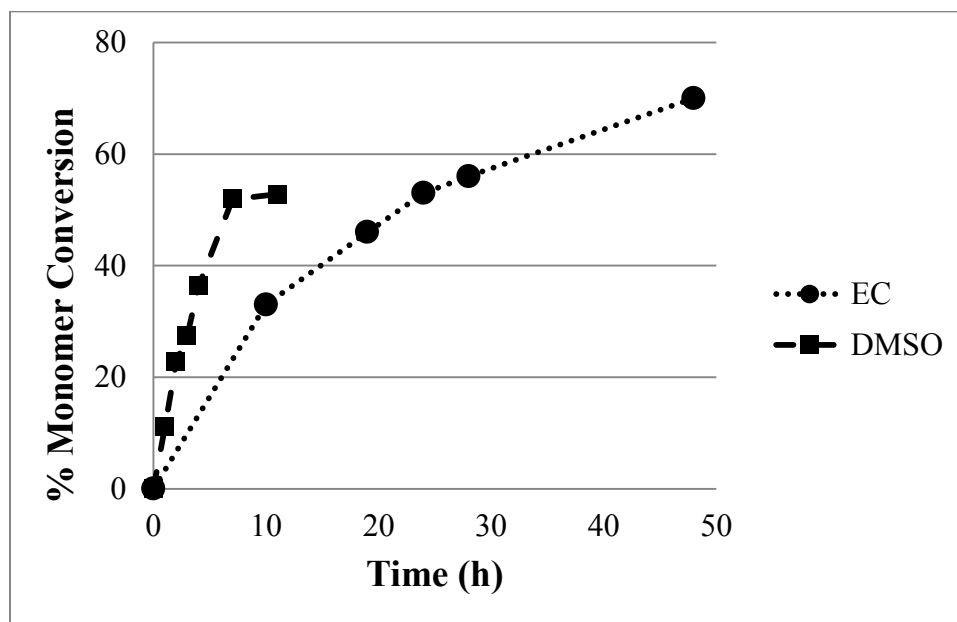


Figure 20. Monomer conversion over time in EC (●) and DMSO (■). Reaction conditions: AN charged 80 wt%, 2400:3:1, CPDB/AIBN, 70°C, 7.4M

It is clear from this data that the rate of copolymerization was much higher in DMSO. The higher conversion in EC when CPDB is used as a CTA is consistent with the results in Reference 21. The chain transfer values are between 0.1 and $0.8 \times 10^{-4} \text{ M}^{-1}\text{s}^{-1}$ for these solvents, and therefore will not have a large effect on the overall rate or conversion. The monomer conversion

difference indicated that EC facilitates propagation, which may be attributed to anti-parallel bonding³⁴ (Figure 21) of the EC to acrylonitrile. EC required several coagulations to fully remove from the copolymers despite its high water solubility.

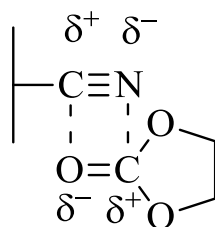


Figure 21. Anti-parallel dipolar bonding between a nitrile and ethylene carbonate

When CMDTC was used as the CTA, the copolymerization rate and conversion in EC and DMSO were comparable as shown in Table 7 and Figure 22.

Table 7. Solvent effect on AN/MA copolymer with CMDTC.

Solvent	CTA/I	Temp (°C)	Time (hrs.)	% Conv	M _{n, calc}	M _{n,NMR}
EC	CMDTC/AIBN	80	6	71	28,700	32,000
DMSO	CMDTC/AIBN	80	6	73	29,500	38,000

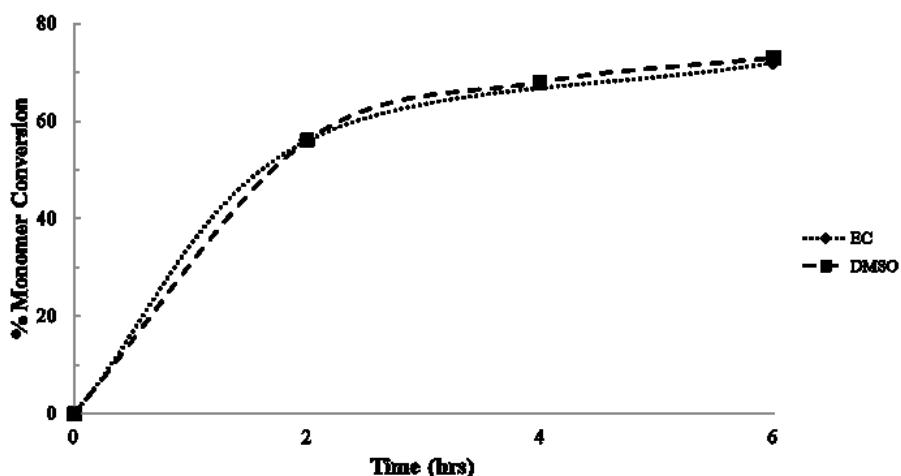


Figure 22. Monomer conversion over time in EC (◆) and DMSO (■). Reaction conditions: AN charged 85 wt%, 2400:3:1, CMDTC/AIBN, 80°C, 4.7M

Because EC was difficult to remove, DMSO was used as the solvent for the majority of this work.

Effect of Concentration

Rate of polymerization in a conventional free radical system is dependent on the concentration of monomer and initiator. Therefore, when the monomer concentration is increased, the rate of polymerization will increase. In conventional free radical copolymerization, it is important to note that for polymers which have solubility limitations, such as PAN, it has been shown that an auto acceleration effect is seen at concentrations greater than or equal to 6 M, much like in bulk reactions. The reaction mixture is thought to form a dilute and a concentrated phase, and the concentrated phase can act like a bulk system which suppresses termination and increases the rate of propagation. At low concentrations, (less than or equal to 2.5 M) the reaction order of the monomer increases from 1 to 1.3-1.5 in DMF and ethylene carbonate respectively.⁴² However, the polymerization rate for a well-designed RAFT system primarily depends on addition and fragmentation rates which occur during the chain equilibration. Therefore, changing the monomer concentration should not have the same impact on rate. A significant increase in the viscosity was observed in these copolymerizations which may affect the conversion. This prompted us to probe concentrations from 2.0 M to 7.5 M, and the results are shown in Figure 23.

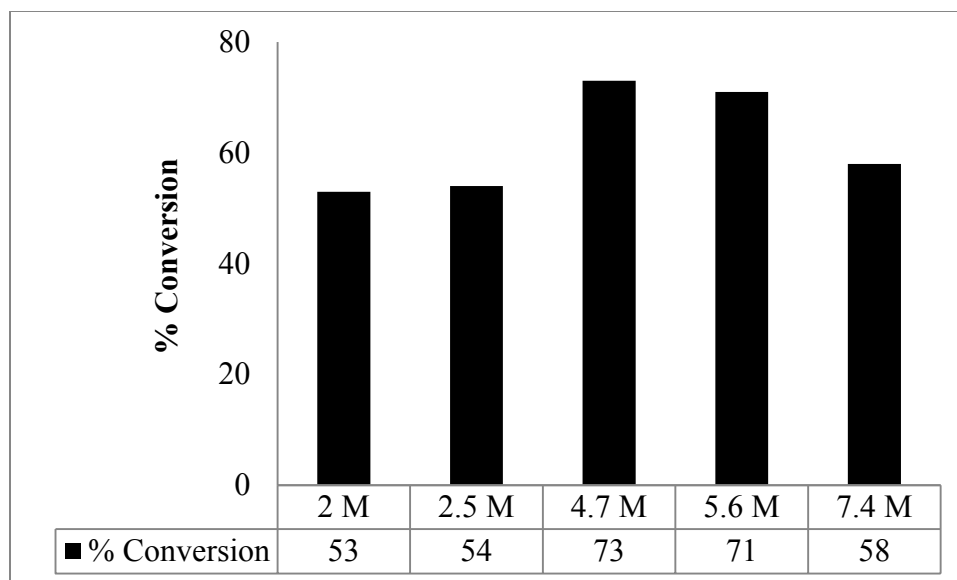


Figure 23. Measured maximum monomer conversion at different monomer concentrations. TCC/AIBN/80°C in DMSO. Reactions were terminated after a maximum conversion was reached.

These data indicate that a moderate concentration allows for higher conversions, and that at dilute and high concentrations the conversion is reduced. The reduced conversion at higher concentrations may be partially explained by a large increase in the solution viscosity. The reduced conversion at the lower concentrations may be due to an increase in the radicals from initiator recombining.⁴²

Effect of Initiator and Temperature

In RAFT polymerization, use of a small amount of initiator is necessary to begin chain growth. These chains react with the chain transfer agent, and β -elimination provides more radicals (see Figure 6, pg. 11). It is useful to select an initiator with a 10 hr. half-life ($t_{1/2}$) near the reaction temperature to ensure radicals are generated at a modest rate throughout the reaction. The $t_{1/2}$, of initiators indicates the amount of time it takes 50% of the initiator to decompose at that temperature. If initiators are used at higher temperatures, the initiator decomposes faster, increasing the concentration of radicals. This is an important fact to remember for RAFT

polymerization, because the control of the reaction depends partially on the radical concentration being kept small.

AIBN is a widely used free radical initiator, and in reports of AN polymerization using homogeneous RAFT polymerization it was the only azo initiator used. Polymerization rate generally increases at higher temperatures, so it is often advantageous to maximize the reaction temperature. Increasing the temperature also increases solubility of the copolymer and reduces the viscosity of the solution allowing for continuous stirring with the magnetic stirrer throughout the reaction. ABCHN, an initiator with a higher $t_{1/2}$, was also studied. ABCHN has not been explored as an initiator in previous AN polymerization using RAFT. Various $t_{1/2}$ of AIBN and ABCHN are shown in Table 8.

Table 8. Reported temperatures for 10 hour, 60 minute, and 10 minute $t_{1/2}$ of AIBN and ABCHN.

$t_{1/2}$	10 hrs	60 min	10 min
AIBN	65°C	82 °C	98 °C
ABCHN	88 °C	102 °C	121 °C

Working with an initiator near its 10 hr. $t_{1/2}$ ensures that the radical concentration will be small at the beginning of the reaction which will minimize early termination reactions. For RAFT copolymerization, keeping the amount of radicals produced from initiator at any one time as low as possible will improve reaction control.

In this study, the initiators, AIBN and ABCHN, were compared at 70, 80, 90 and 100°C. This data is shown in Table 9.

Table 9. Experimentally measured % monomer conversion. Reaction conditions: 85/15, 2400:3:1, 4.7M

Entry	CTA	Initiator	Temp (°C)	Wt. % AN	% Conv	M _{n,calc} g/mol	M _{n,NMR} g/mol
1	CPDB	AIBN	70	88	51	20,400	27,300
2	CPDB	AIBN	80	85	55	22,000	23,800
3	CPDB	ABCHN	90	88	49	19,600	32,600
4	CPDB	ABCHN	100	86	56	22,400	29,000
5	CMDTC	AIBN	70	85	79	31,600	25,800
6	CMDTC	AIBN	80	87	73	29,200	38,000
7	CMDTC	ABCHN	80	87	75	30,000	41,000
8	CMDTC	ABCHN	90	85	84	33,600	43,900
9	CMDTC	ABCHN	100	86	86	34,400	39,000

Performing a polymerization at higher temperatures will increase k_p and k_i which should improve conversion. The conversions were higher from materials made using ABCHN because the initiator $t_{1/2}$ at each reaction temperature of ABCHN was longer than AIBN. Therefore, a steady concentration of radicals was produced throughout the reaction. When a large concentration of radicals is produced, termination reactions are more likely at the early stages of the reaction. Early termination reactions may involve recombination of the radicals produced from the initiator and combination reactions of low molecular weight species. Even when a RAFT agent is used, a large number of radicals will cause the reaction to be less controlled.

Effect of RAFT Chain Transfer Agent

Cyanopropyl dithiobenzoate (CPDB) and cyanomethyl dodecyl trithiocarbonate (CMDTC) were examined as appropriate chain transfer agents for the AN and MA copolymerization. The copolymers with end groups from CPDB and CMDTC are shown in Figure 24.

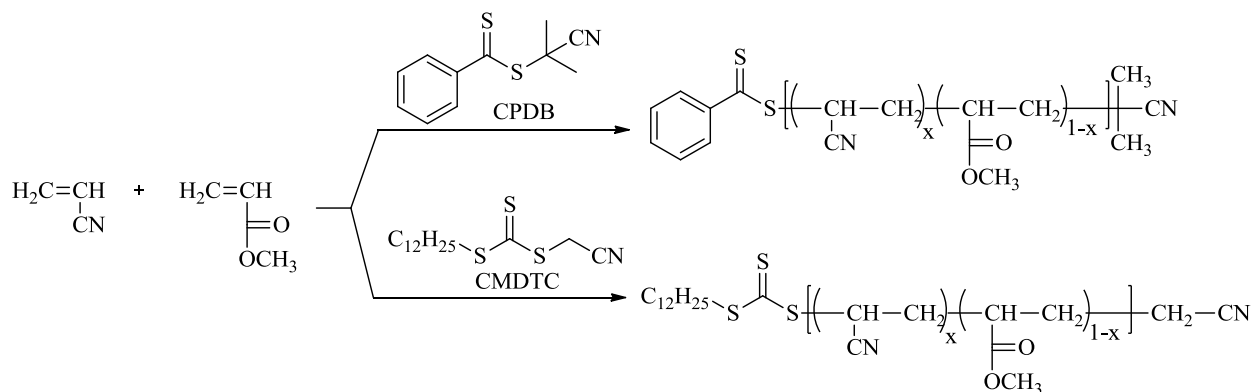


Figure 24. Expected structure of copolymer synthesized by RAFT using CPDB and CMDTC as the CTA

These RAFT CTA's were compared at several different temperatures using both initiators. Several examples are shown in Table 9. CPDB has been shown to control AN polymerization in several studies,^{19,20,21,23} however, CMDTC has not been explored as a suitable CTA for polymerization of AN. Table 9 shows that copolymers synthesized using CPDB had lower conversion than those made with CMDTC which may be due to several factors. The dormant radical species formed from CPDB is dithiobenzyl radical, which is resonance stabilized through the aromatic ring. Since the dithiobenzyl radical is stabilized, the dormant radical species is persistent and has been shown to undergo cross termination reactions with other small radical species. Cross termination reactions lower the concentration of radicals as well as available chain transfer agent. Since AN and MA radicals are highly reactive and the dormant radical species is relatively stable, cross termination reactions may occur especially when there are a high concentration of radicals from initiator. The dormant radical species for CMDTC is a dodecyl trithiocarbonyl radical which is not as persistent, so the higher conversion is due to the copolymer chains remaining active longer than those of CPDB.

Qualitative Kinetic Information from $^1\text{H-NMR}$

In RAFT (co)polymerization, a good indicator of the reaction control is the monomer conversion over time, which can be monitored by taking aliquots of the reaction mixture over time and using $^1\text{H-NMR}$ to measure conversion. In an ideal controlled free radical polymerization, the monomer conversion will increase at the same rate over time until 100% conversion is reached. The rate of this increase depends largely on the rate constant of addition, k_{addP} , and fragmentation, k_{-addP} , which are mechanistically shown in Figure 6 (pg. 11).

In Figure 25, the monomer conversion over time for several copolymers made with CPDB is shown.

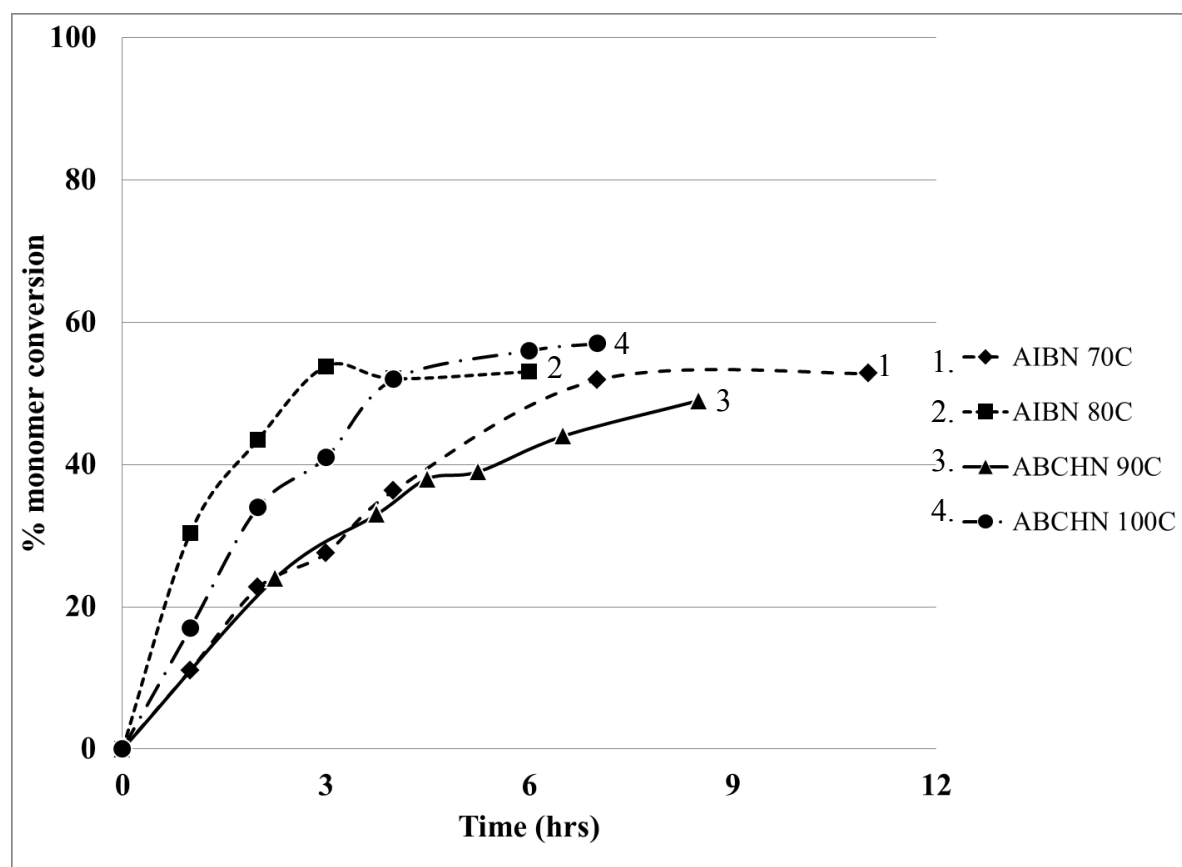


Figure 25. Time vs. % monomer conversion measurements for RAFT copolymers using CPDB as the CTA. Reaction conditions: 85/15, 2400:3:1, 4.7M

It is important to note in all reactions using CPDB and DMSO, the maximum monomer conversion was below 60%. Since increasing the monomer conversion was a primary thrust of this work, an explanation of why conversion remained low should be discussed.

In Figure 25, the reaction temperature for example 1 and 3 was close to the 10 hr. $t_{1/2}$, so radical availability over the reaction time would not be an issue. The conversion proceeded in a relatively linear fashion during the first four hours of the reaction, however after approximately 4 hours the reaction rate began to slow in both, indicating the reaction kinetics were changing. It is also interesting to note that the slope of the lines formed by these reactions were nearly identical, indicating that the rate of polymerization was similar for these two reactions.

In Figure 25, example reactions 2 and 4 were performed at temperatures that were near the 1 hr. $t_{1/2}$ for these initiators, so the concentration of initiator derived radicals would be high initially. This could lead to a large number of chains growing from initiator instead of chain transfer agent, which means the copolymerization was not well-controlled. The conversion rapidly increased then abruptly leveled off, indicating a significant change in the reaction kinetics after less than 3 hours reaction time.

When the examples in Figure 25 are examined from an initiator perspective, a straightforward explanation would be that there are no radicals available to continue the copolymerization when the conversion levels off. It is important to remember that RAFT polymerization theoretically needs a small amount of initiator derived radicals to activate the RAFT agent. Likewise, if the low conversion was due to lack of radicals, this would indicate that amount of termination reactions was significant. In cases 1 and 3, there should not be a large concentration of active radicals at any point during the copolymerization, so the low conversion would not be termination related. For 2 and 4, termination may be more of an issue

because of high radical concentrations. The chromatograms from SEC may be able to provide insight if termination by combination is an issue since the materials will be higher molecular weight, and this will be discussed later.

From a CTA perspective, the dormant radical of CPDB is a dithiobenzoate radical which is highly resonance stabilized leading to a long lifetime due to a high k_{addP} compared to k_{-addP} . The long lifetime of the radical makes it prone to cross-termination reactions with other small radical species (see Figure 8, pg. 14), causing retardation at the beginning of the copolymerization which reduces the amount of RAFT agent and radicals. Radicals produced from initiator throughout the reaction may react with the dormant radical species causing cross termination and reaction slowing.

A third possibility for the reduced conversion with the use of the CPDB CTA is that the active radical species did not persist for long enough to add another monomer especially as the monomer concentration decreased and solution viscosity increased. This seems to be the most logical explanation because the conversion slows gradually with a relatively large amount of monomer remaining.

A reaction between CPDB and ABCHN at 80°C failed to produce copolymer. At 80°C, this initiator is below its 10 hr. $t_{1/2}$. This shows that k_d of ABCHN at 80°C does not produce enough radicals to overcome retardation and begin propagation.

Figure 26 shows % monomer conversion vs. time when CMDTC is used as the RAFT CTA.

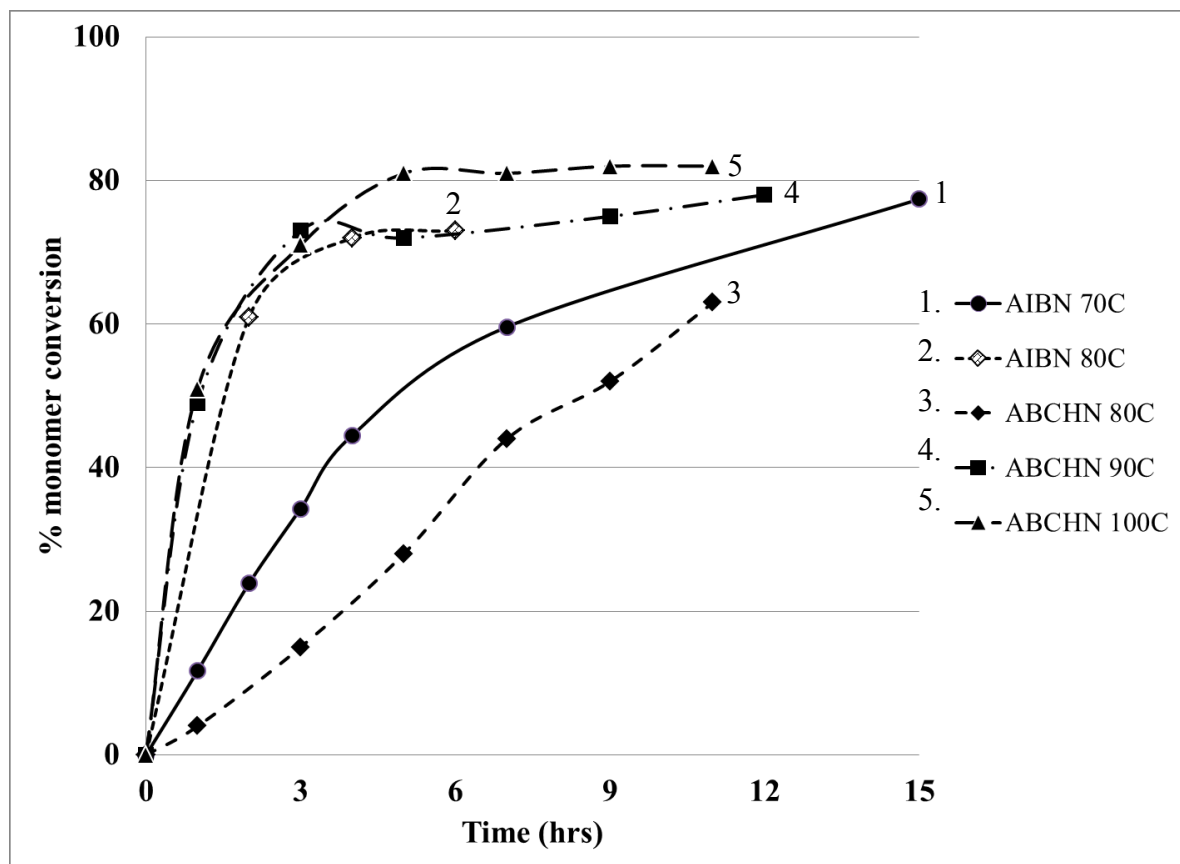


Figure 26. Time vs. % monomer conversion measurements for RAFT copolymers using CMDTC as the CTA. Reaction conditions: 85/15, 2400:3:1, 4.7 M

Monomer conversions of over 80% can be reached using CMDTC, however slowing or stopping of the monomer conversion is still observed which is undesirable if 100% conversion is to be reached. In Figure 26, example reactions 1, 3, and 4 were all performed at temperatures at or below the 10 hr. $t_{1/2}$ of the initiator. Examples 1 and 3 showed linear growth over time as expected from the RAFT mechanism, but 4 grew quickly over a short time period. The fast growth does not necessarily mean it was not controlled, but it speaks to the rapid k_p of AN and MA. At this temperature, the k_p and k_{tr} values may not be well balanced and propagation is favored over equilibration despite a low radical concentration. In Figure 26, examples 2 and 5 were performed at temperatures near the 1 hr. $t_{1/2}$, and as discussed previously it is not surprising that the conversion is fast in these cases.

Based on this data it is unknown what the most likely explanation is for the slowing of the monomer conversion in the reactions which appear to be controlled, 1 and 3 (Figure 26). As with CPDB, it again may be explained best by the active chains not persisting long enough to continue propagation. The monomer conversion was higher than copolymers made with CPDB because the k_{addP} is slower, so the copolymer chains were active for longer allowing for propagation to continue for longer but high solution viscosity and decreasing monomer concentration may stop the copolymerization.

The highest percent monomer conversion reached in this work was 86%, using CMDTC and ABCHN at 100°C. Monomer conversions up to 86.3%³³ have been reported in the published literature for an AN homopolymers synthesized by RAFT. However, incorporation of 5% MA as a comonomer caused a reduced monomer conversion from 73.5% (AN homopolymer) to 46.3% when the CPDB and AIBN were used as the CTA and initiator.²¹ Use of CMDTC and ABCHN provides a much improved monomer conversion for this copolymerization.

Molecular weight determination

The viscosity of a polymer solution can be related to its viscosity molecular weight (M_v) using the Mark-Houwink-Sakurada equation (Equation 6).

$$[\eta] = KM_v^a$$

Equation 6. Mark-Houwink-Sakurada equation

where $[\eta]$ is the intrinsic viscosity, and K and a are constants which depend on the polymer, solvent and temperature. $[\eta]$ is defined as the viscosity of the polymer in solution as it approaches zero concentration. This is measured by extrapolation of the inherent and reduced viscosities to zero concentration. The inherent and reduced viscosities are measured at several

concentrations, and the lines formed from these points should intersect on the y axis. This intercept is $[\eta]$. An example of this type of plot is shown in Figure 27.

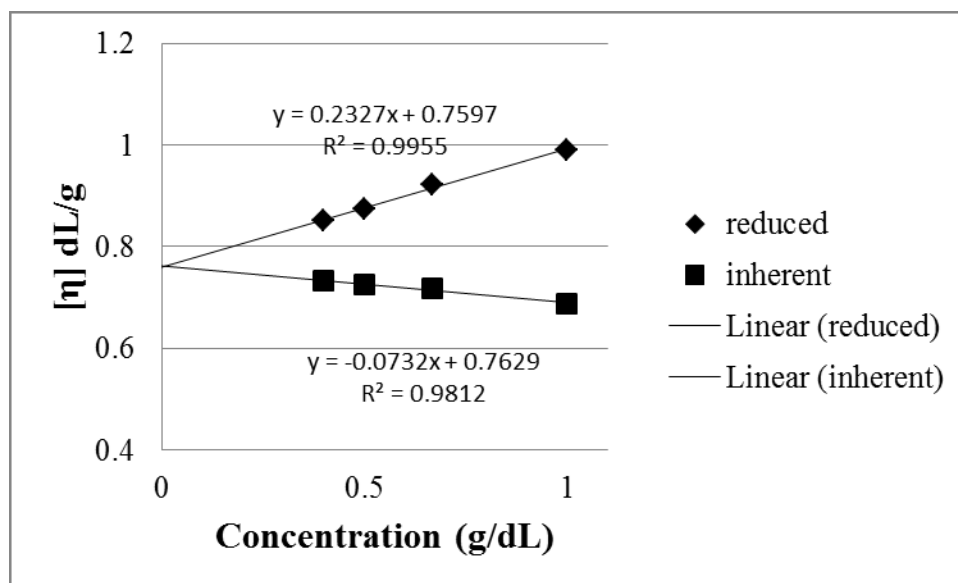


Figure 27. Example plot for intrinsic viscosity determination

The intrinsic viscosity used for these copolymers was the average of the y-intersect, or b value from the linear equations. It is important to note that the K and a values used were for a PAN-stat-MA that was a 91.5/8.5 w/w.⁴⁰ Therefore the K and a values used may not be directly applicable to copolymers with differing compositions from the reference.

SEC was used to measure M_n and M_w . The mathematical expressions for molecular weight are shown in Figure 28, where M_i is a molecule of mass i, and N_i is the number of molecules of M_i .

$$M_n = \frac{\sum M_i N_i}{\sum N_i} \quad M_w = \frac{\sum M_i^2 N_i}{\sum M_i N_i} \quad PDI = \frac{M_w}{M_n}$$

Figure 28. Mathematical expression for molecular weights

M_n is the weighted mean molecular weight based on the number of molecules. Therefore, this value represents the highest population of the molecular weights. M_w is the weighted mean molecular weight based on the molar mass of the molecules. This value favors the higher

molecular weights. The PDI, or polydispersity, is a measure of the distribution of molecular weights, and a value of 1 indicates that all the polymer chains are equal in length.

The stationary phase used in SEC is made of beads with different pore sizes. The pores in the beads allow for separation of polymer molecules based on their hydrodynamic volume, with higher molecular weights eluting first because they cannot penetrate into the pores of the beads. As the polymer elutes, the molecular weight fractions flow through different detectors which provide some information which can be used to determine molecular weight. For these copolymers, three detectors were used, a refractive index (RI) detector, a viscosity detector, and a light scattering (LS) detector. The RI detector measures the change in the refractive index compared to that of the solvent. The viscosity detector provides information about the concentration. The light scattering detector measures the scatter of polymer in solution vs. that of the solvent.

For these copolymers, two different methods were used for molecular weight measurement, universal calibration and light scattering. Based on narrow molecular weight distribution polystyrene standards of known molecular weights, a universal calibration curve was used to calculate M_n , M_w and PDI. The light scattering detector was used to measure the absolute M_w based on a dn/dc value (the change in refractive index as the concentration changes) of 0.0500.

Figure 29 shows the molecular weight data and chromatograms from SEC for PAN-co-MA in which the chain transfer agent was varied.

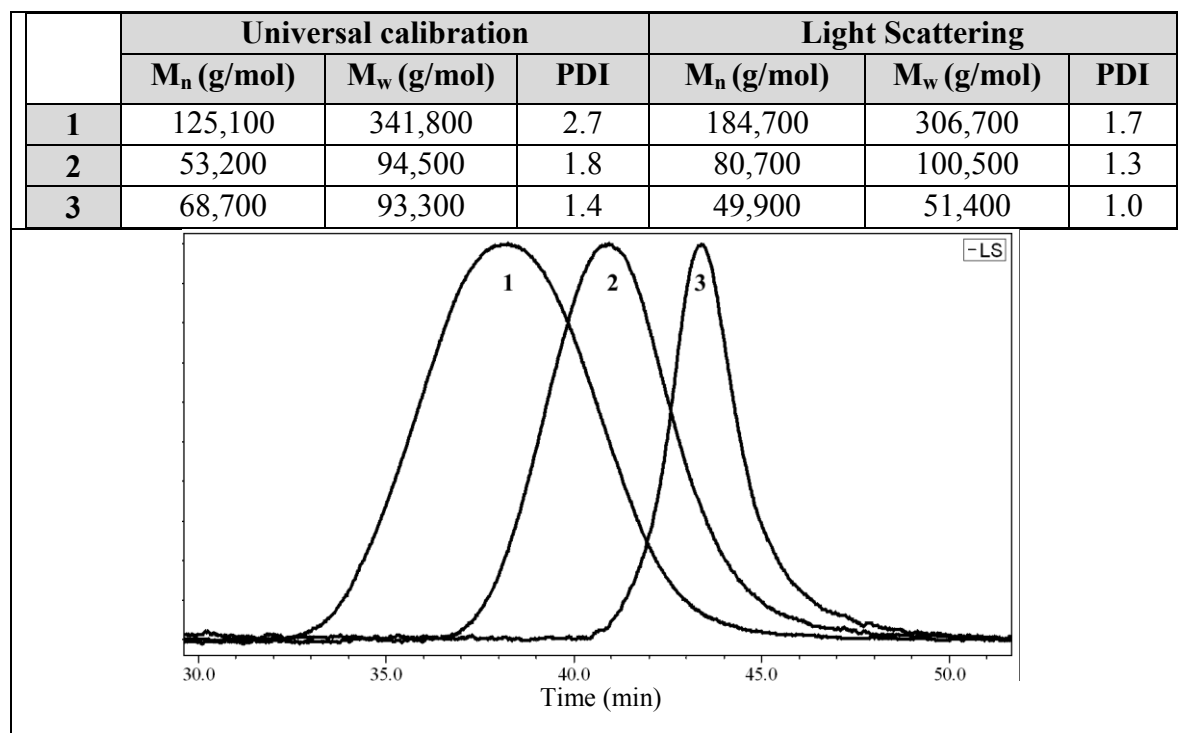


Figure 29. (1) No chain transfer agent (2) dodecanethiol (3) CPDB. All reactions were run at 4.7M in DMSO at 80°C with AIBN as the initiator. (2) and (3) used a 2400:3:1 M:CTA:I ratio.

When no CTA is used (Figure 29, (1)), the copolymerization is fast and the magnetic stirring stops in less than one hour. Without CTA, high molecular weight and broad polydispersity materials are formed because chain growth is limited only by termination. Addition of dodecanethiol (Figure 29, (2)) as a chain transfer agent reduces the molecular weight and PDI significantly; however the reaction remains very fast and stops stirring in less than 1.5 hours. When CPDB (Figure 29, (3)) is used, the reaction proceeds over a 6 hour time period. This shows that the addition of the RAFT CTA slows the rate of copolymerization significantly and allows for the copolymerization to be controlled as evidenced by a lower PDI.

The $M_{n,NMR}$ from the samples in Table 9 were compared to molecular weights from SEC calculated from universal calibration and light scattering, as well as the viscosity molecular weight (M_v) calculated from $[\eta]$. This is shown in Table 10.

Table 10. Comparison of molecular weight data 1H-NMR, SEC, and intrinsic viscosity from Table 9, Entries 1-9.

Table 9, Entry	$M_{n,NMR}$ g/mol	Universal calibration			Light Scattering			M_v g/mol
		M_n g/mol	M_w g/mol	PDI	M_n g/mol	M_w g/mol	PDI	
1	27,300	33,000	43,000	1.3	49,000	52,000	1.1	35,000
2	23,800	30,500	44,600	1.5	38,600	41,400	1.1	38,000
3	32,600	30,500	47,000	1.5	32,900	34,700	1.1	37,000
4	29,000	33,200	50,200	1.5	32,800	34,600	1.1	37,000
5	25,800	38,200	64,200	1.7	39,600	46,500	1.2	52,000
6	38,000	57,000	83,000	1.5	62,000	66,000	1.0	55,000
7	41,000	46,000	65,000	1.4	61,000	76,000	1.2	60,000
8	43,900	39,000	60,000	1.5	58,000	65,000	1.1	61,000
9	39,000	41,000	61,000	1.5	56,000	64,000	1.1	53,000

The precision of the $M_{n,NMR}$ depends on the identification of the end groups and assumes that each copolymer has two end groups. The $M_{n,NMR}$ values are very dependent on the shape of the integral and the value it is set, so small deviations in the end group lead to large differences in the molecular weight measured by NMR. This effect will be more pronounced as the chain length increases, and therefore the $M_{n,NMR}$ is unreliable as the molecular weight increases.

The molecular weights from universal calibration are measured from a polystyrene universal calibration curve. This curve plots the $\log [\eta]*[M]$ versus the retention time of polymers with known molecular weights. Since a polymer unknown has a unique $[\eta]$ and retention time, the molecular weight can be determined using the calibration curve.

The light scattering molecular weights depend on the incident scattered light, dn/dc value, and sample concentration. If the dn/dc and concentration are correct then the absolute molar mass can be calculated. For these AN copolymers, the dn/dc value determined from batch

measurements was 0.050 for the NMP/LiBr elution solvent. This relatively small dn/dc value means that the changes in refractive index versus concentration are subtle, which can make the dn/dc determination difficult. Since light scattering only looks at hydrodynamic volume of the molecules in solution, it gives an average of this size and the larger molecules are weighted more. Therefore, the lower molecular weight molecules are not counted as much, and the M_n values are artificially high resulting in lower PDIs.

The reported M_v values are based on parameters from a 91.5/8.5 w/w PAN-co-MA. The materials reported in Table 10 have less AN, so the chains are less rigid because the MA will break up the dipolar interactions between the nitriles, which will improve solubility. Higher solubility will decrease the a constant for the Mark-Houwink-Sakurada equation. A smaller a will increase the calculated molecular weight, so it is likely that the M_v reported in Table 10 are lower than the actual M_v .

For the samples in Table 10, the light scattering, universal calibration, and intrinsic viscosity molecular weights for these samples all agree fairly well, despite the potential errors due to the measurements which have already been discussed.

Despite assumptions made in the calculations, if a polymerization is controlled, the molecular weight over time will increase linearly. An example of this for this system is shown in Figure 30 and Figure 31.

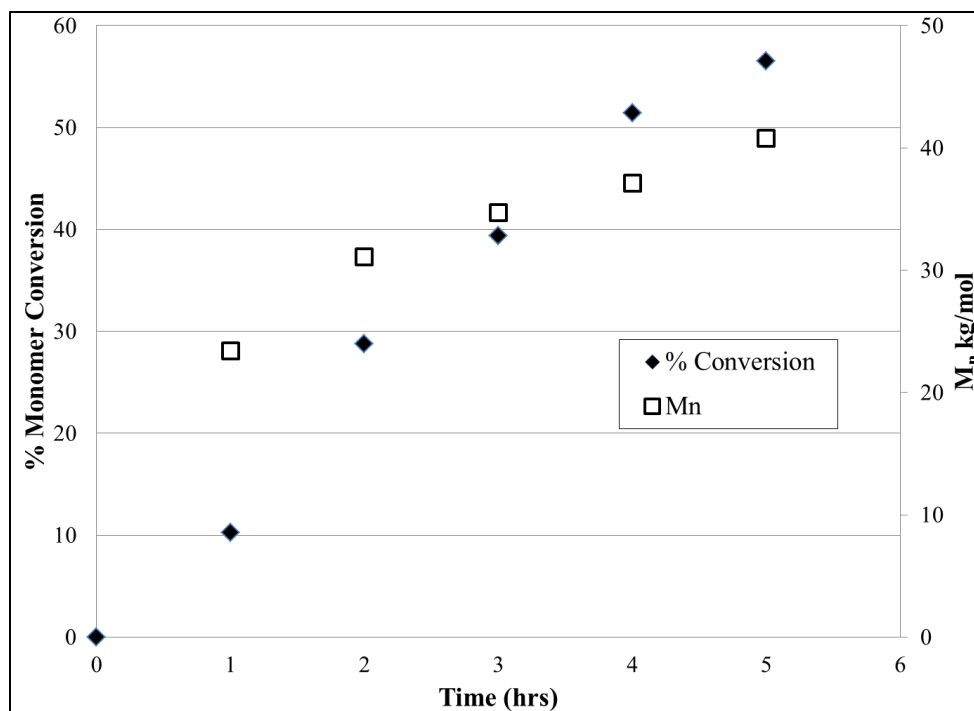


Figure 30. Monomer conversion vs. time (◆) and M_n from universal calibration (□) from 1 to 5 hours. Reaction conditions: 85/15, 2400:3:1, CPDB/AIBN, 80°C, 4.7M

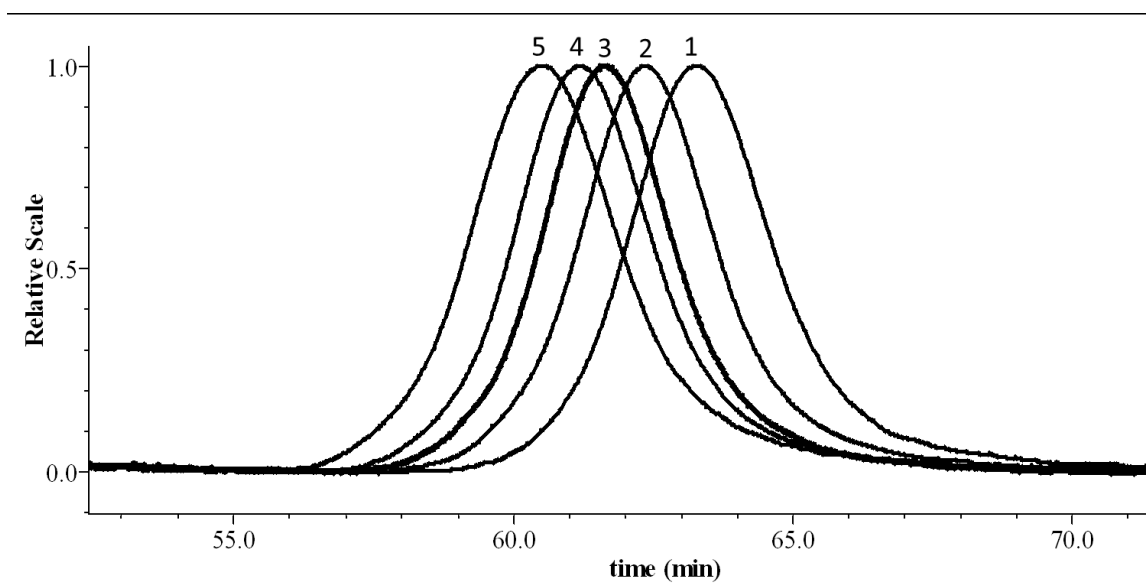


Figure 31. SEC light scattering traces from the data in Figure 30. The numbers above the curve represent the samples at time 1 through 5 hours.

In Figure 30, the % monomer conversion and M_n from universal calibration are shown from samples taken at 1, 2, 3, 4 and 5 hours. Both the monomer conversion and M_n increase linearly

over this time frame as expected for a controlled copolymerization. Figure 31 shows the SEC traces from light scattering. The retention time of the copolymer decreased as the reaction proceeded, indicating that higher molecular weight materials were eluted. This data indicates that the copolymerization was controlled.

Measuring T_g , T_m , and T_d of RAFT PAN-co-MA materials

Differential scanning calorimetry (DSC) was used to measure the T_g , T_m , and T_d of PAN-co-MA materials. DSC measures the change in the sample enthalpy over time, dH/dt , over a set temperature program, dT/dt . This will give the specific heat capacity, dH/dT , which is related to transition temperatures. T_g is the temperature where the amorphous regions of the polymer change from glassy to rubbery. This transition is caused by an increase in segmental motion of the copolymer, and causes a step change increase in the heat capacity. T_m is the temperature where the crystalline portion of the polymer begins to melt. This produces an endothermic peak that will increase in area as the crystalline fraction of the copolymer increases.¹⁴ T_d is the temperature where chain degradation begins. This process is exothermic.

For copolymers, the Fox equation⁴³ (Equation 7) can be used to predict the T_g using the homopolymer values, $T_{g,1}$ and $T_{g,2}$, if the weight fraction is known.

$$\frac{1}{T_g} = \frac{W_1}{T_{g,1}} + \frac{W_2}{T_{g,2}}$$

Equation 7. Fox equation; T_g values are in K

Figure 32 shows DSC thermograms and the transition temperatures for a series of copolymers with AN incorporation that varies from 82/18 to 95/5 AN:MA.

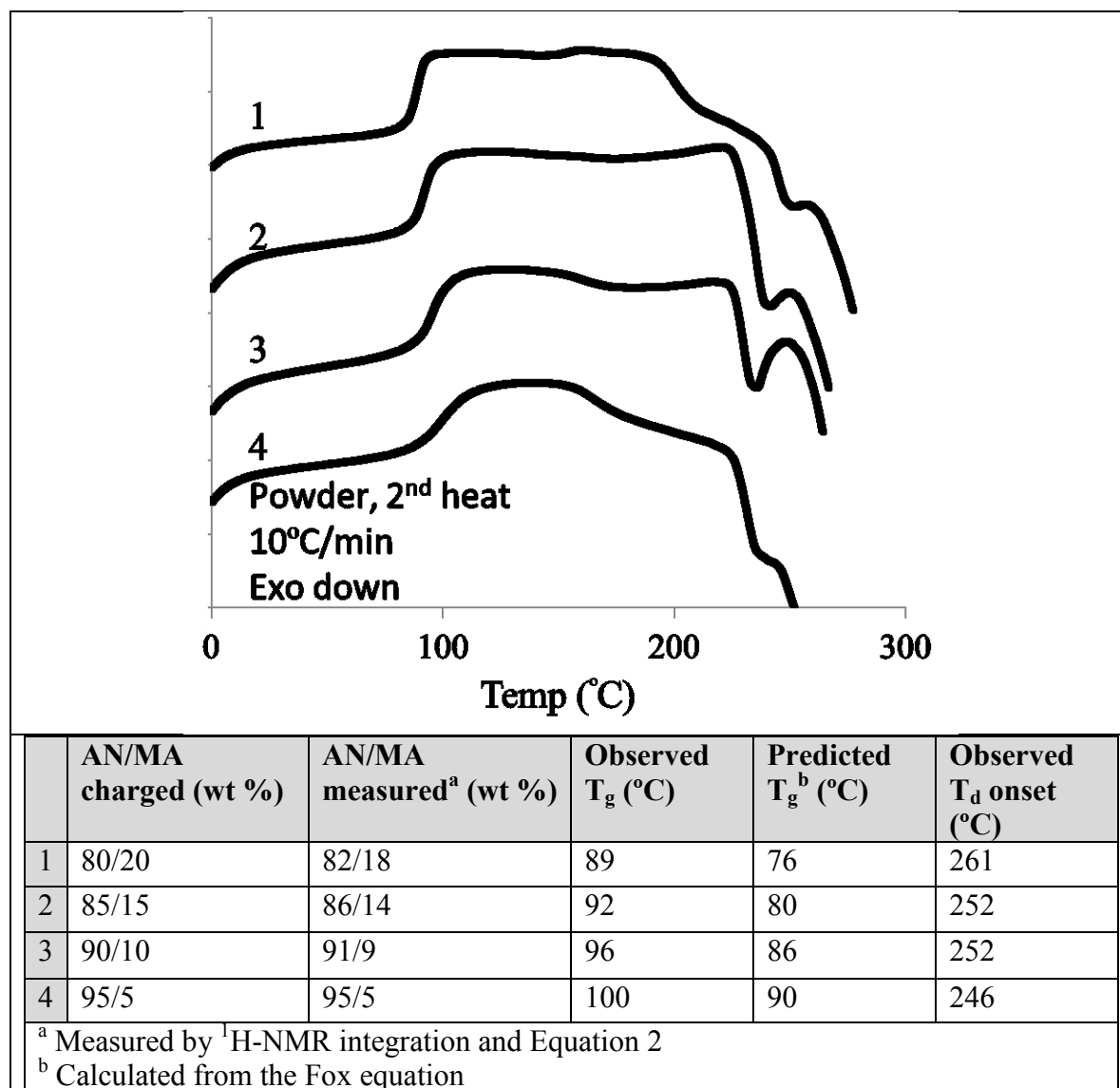


Figure 32. DSC of PAN-co-MA copolymers. Reaction conditions: 2400:3:1, CPDB/AIBN, 70°C, 7.4M in EC. The M_w from LS was between 45000 and 50000 for these samples.

Using Equation 7, with T_{g,AN} as 95°C⁴⁴ and T_{g,MA} as 5°C,⁴⁵ the copolymer T_g's can be predicted. The T_g's were observed to be an endothermic step change transition in the thermograms which increased in temperature with the AN content. In these samples, T_m's were not observed, however the T_d was higher at higher MA content, indicating that there was a disruption of the strong nitrile interaction. In each of these examples, there was an endothermic hump after degradation had begun. This transition may be linked to the RAFT agent, CPDB. To test if the

RAFT agent is responsible for this transition, CPDB was removed via reduction with Bu_3SnH (Figure 33).

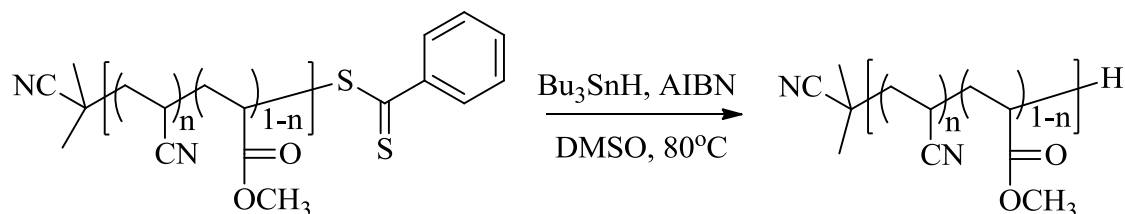


Figure 33. Reduction of dithiobenzoate end group with Bu_3SnH

As shown in Figure 34, $^1\text{H-NMR}$ confirms that the dithiobenzoate end group was removed.

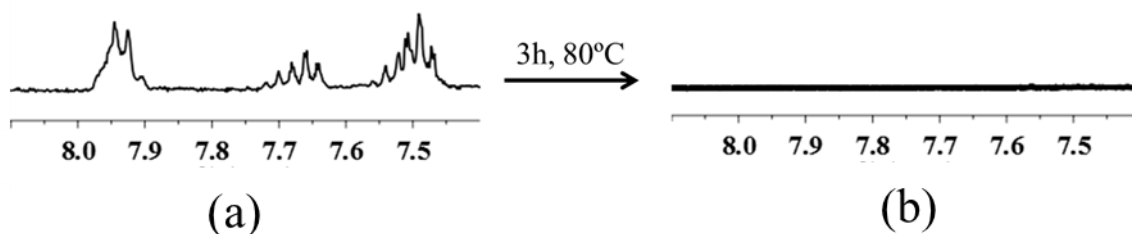


Figure 34. $^1\text{H-NMR}$ of copolymer before (a) and after (b) removal of the dithiobenzoate end group.

The copolymer appearance changed from pink to white, which indicates end group removal. The chromatograms and molecular weight measurements from SEC (Figure 35) show that the molecular weights from SEC before and after end group removal were within experimental error. The lower PDI after end group removal may be due to removal of low molecular weight material after precipitation for product isolation.

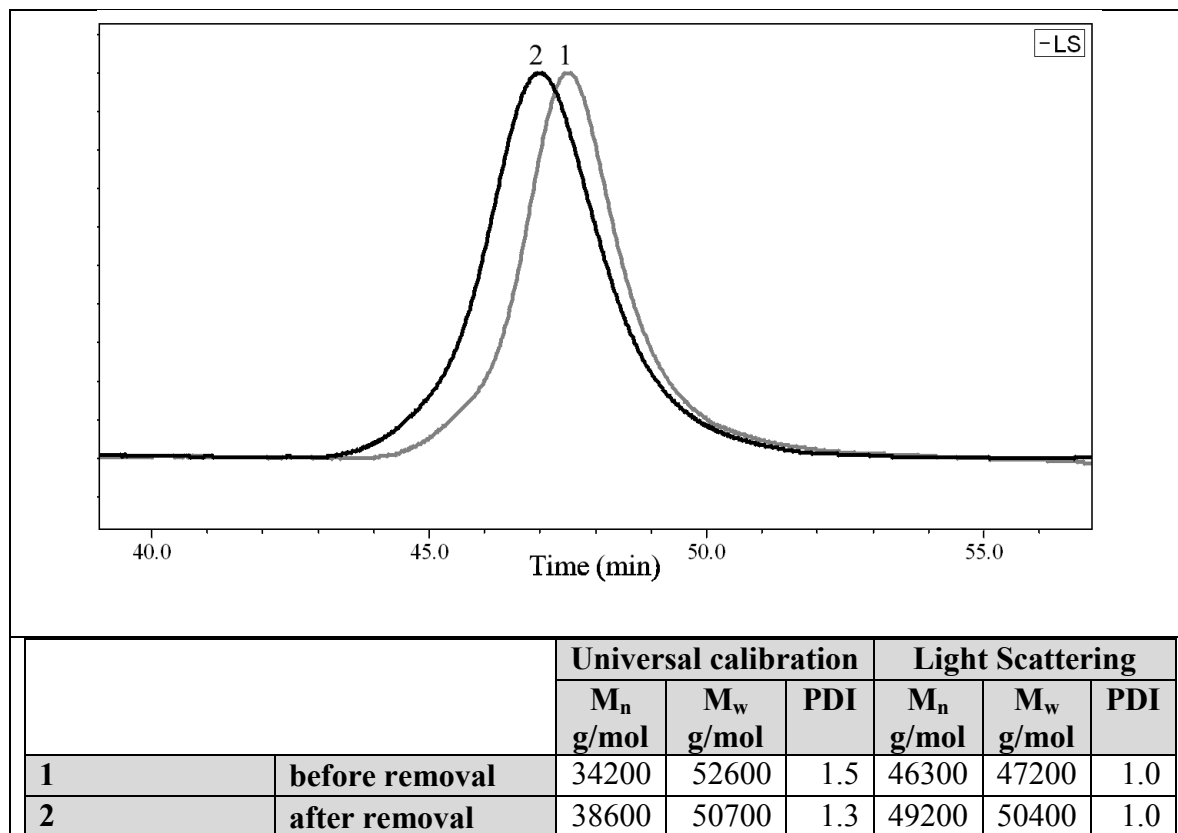


Figure 35. SEC LS trace from before (1) and after (2) end group removal and molecular weight data from universal calibration and light scattering

Figure 36 shows the thermograms from DSC before and after end group removal. The small endothermic hump disappears after the end group was removed from the copolymer. In this sample, it is clear that there was an endotherm after the T_g , indicating there was some crystallinity in this sample which begins to melt at 260°C.

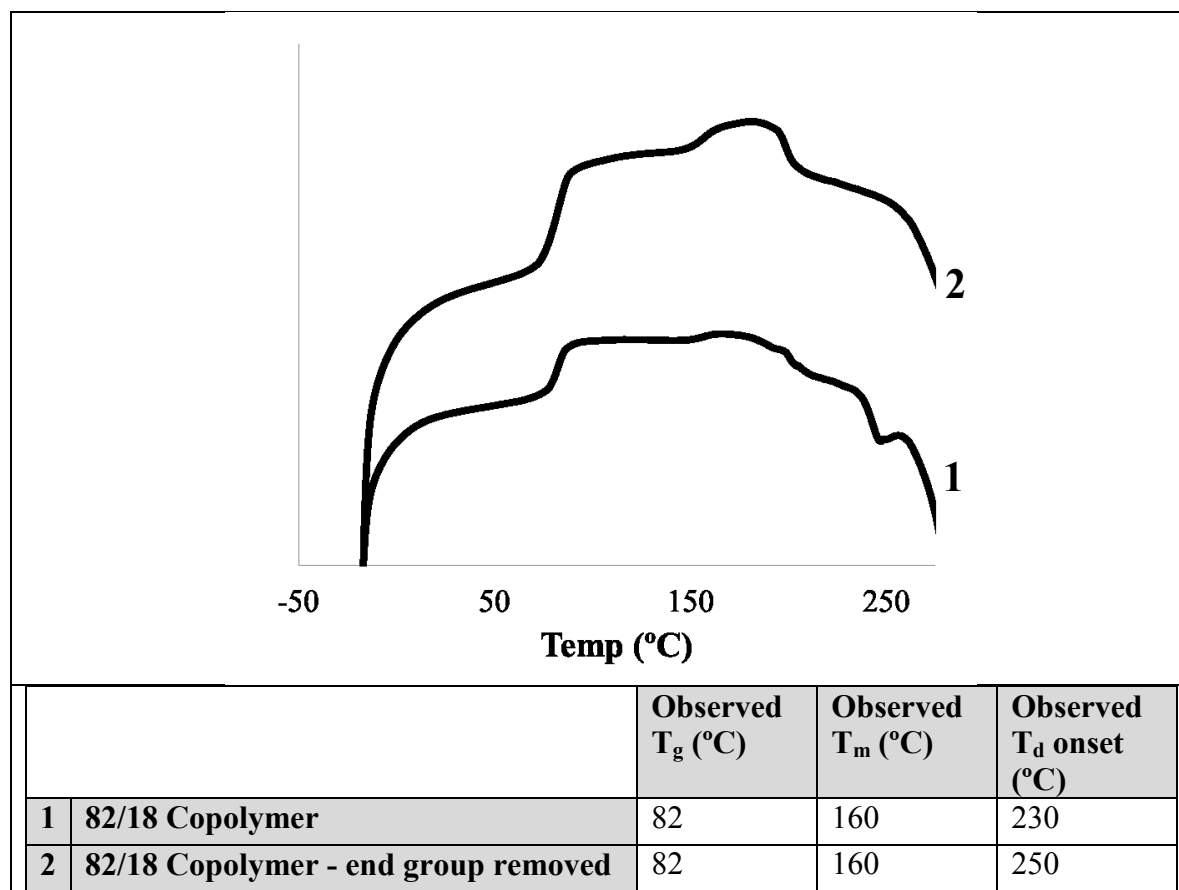


Figure 36. DSC before (1) and after (2) end group removal. Conditions: 2nd heat, 10°C/min, powder, exo down.

Since the majority of the copolymers discussed in this thesis were higher AN content and were synthesized in DMSO, DSC was used to obtain thermograms for copolymers synthesized with CPDB and CMDTC (Figure 37). Interestingly, use of DMSO as the solvent eliminates the endothermic hump which was seen after the onset of degradation (see Figure 36, (1)). This indicates that this transition is due to EC and not the end group, and it may be a result of EC being released from the copolymer as a gas. It was previously discussed how tightly the EC binds to AN, and the boiling point of this solvent is 260°C, which is in the range of this transition. The transition disappearing after end group removal was probably due to the work-up of the copolymer via precipitation removing the residual EC and not removal of the dithiobenzoate end group.

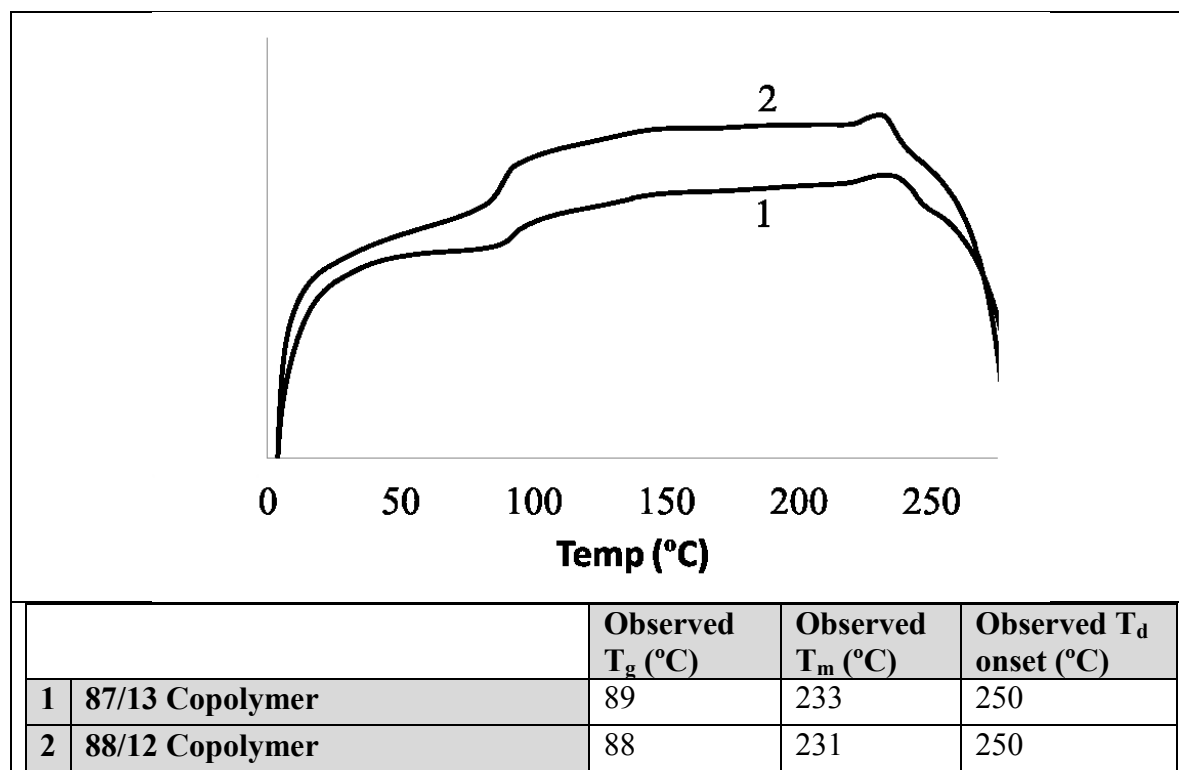


Figure 37. (1) 85/15, 2400:3:1, CPDB/AIBN, 80°C in DMSO at 7.4 M (2) 85/15, 2400:3:1, CMDTC/AIBN, 80°C in DMSO at 4 M

As discussed previously, the T_g of the higher AN content copolymers is higher than that of the 82/18 copolymers. There is also a distinct endotherm before degradation observed in these samples which was identified as the T_m . This T_m occurred 70°C higher at this composition versus that of the 82/18 (Figure 36) indicating the significance of the AN content to the higher degree of order being produced in AN/MA copolymers. Ideally, for this AN/MA composition to be melt processed, the T_m would need to be lowered further. Previous work in the McGrath group showed that a 88/12 PAN-co-MA synthesized by suspension copolymerization was shown to have a stable melt viscosity at 220°C for about 20 minutes by parallel plate rheology, indicating this composition may be the upper limit to a stable melt-processible PAN copolymer.¹²

To illustrate melt processibility, an 82/18 PAN copolymer was melt pressed between two steel plates at 190°C (Figure 38). The orange color of the film is due to the RAFT agent, CPDB. The film is transparent which indicates that this sample is amorphous.



Figure 38. Film melt pressed at 190°C from an 82/18 PAN-co-MA.

Chapter V: Conclusions

Two RAFT agents, CPDB and CMDTC, were successfully used to synthesize high molecular weight AN/MA copolymers, as evidenced by the SEC and IV data. Use of these RAFT agents, along with the initiators AIBN and ABCHN, produced PAN-co-MA with PDIs below or equal to the copolymers made using conventional free radical polymerization. EC and DMSO were determined to be suitable solvents for the copolymerization reactions, and monomer concentrations close to 4.7 M had the best percent monomer conversion. The percent monomer conversion generally increased as the reaction temperature was increased. Based on the kinetic data, the overall rate of the copolymerization was higher when CMDTC was used as the RAFT CTA. Use of CMDTC also had higher percent monomer conversion versus that of CPDB. The highest monomer conversion, 86%, was achieved at 100°C when CMDTC and ABCHN were used as the CTA and initiator for the copolymerization.

Thermal analysis showed that the T_g , T_m , and T_d are reduced upon incorporation of greater amounts of MA. Removal of the dithiobenzoate RAFT end group did not produce a significant change in the thermal transitions. A T_m was seen in an 88/12 wt% AND 82/18 wt% PAN-co-MA at approximately 230°C and 160°C, respectively. In the 82/18 wt% PAN-co-MA, the T_m was eliminated or sufficiently low for the copolymer to be melt-pressed into a film.

Chapter VI: Suggested Future Research

The study reported in this thesis involving the copolymerization of AN and MA by RAFT polymerization could be further refined by assessing higher ratios of RAFT CTA to initiator, such as 5:1 or 10:1, while keeping the total monomer concentration the same. This would decrease the amount of initiator derived end groups and should provide more control in the polymerization. In this work, monomer conversions up to 85% were reached. It would be useful to do rigorous kinetic measurements to determine rate of polymerization, conversion, and control. Since higher temperatures generally resulted in higher conversions, use of an initiator with a higher temperature half-life may help to improve the conversion without adding an excess amount of radicals. However, to maintain control of the copolymerization at higher temperatures, use of a dithiocarbonate may be necessary. Selection of a dithiocarbonate that is not benzyl stabilized may provide improved conversions and copolymer control. Also, copolymerization of vinyl acetate with AN using RAFT should also be investigated since it is used in many commercial applications as the comonomer due to reduced cost over MA.

Further research could be done on the PAN-co-MA materials synthesized in this thesis to determine if melt processibility is viable by using thermal characterization to determine if the T_m is below 200°C. If melt processibility seems to be a viable option, use of capillary or parallel plate rheology can be used to determine melt-stability. If the T_m is above 200°C, addition of a plasticizer may allow for the T_m to be lowered to below 200°C.

Once melt processibility is determined, an additional area of research would be to compare the melt-processible PAN-co-MA materials synthesized by RAFT with copolymers made using conventional free radical polymerization to determine if there is an advantage to using RAFT copolymerization. Since most of the commercial PAN copolymers are made using

suspension copolymerization, using suspension to make the RAFT copolymers may provide more insight into the viability and adaptability of using controlled over conventional materials.

References

1. Gadecki, F. A., *Acrylic Fiber Technology and Applications*. Marcel Dekker, Inc.: New York, New York, 1995.
2. Aizenhtein, E. M., *Fibre Chemistry* 2009, 41 (5), 281-293.
3. Moad, G.; Rizzardo, E.; Thang, S. H., In *Polymer Science: A Comprehensive Review*, Matyjaszewski, K., Ed. Elsevier: 2012; Vol. 3, pp 181-225, and references therein.
4. Destarac, M., *Macromolecular Reaction Engineering* 2010, 4 (3-4), 165-179.
5. Limberg, C., The SOHIO Process as an Inspiration for Molecular Organometallic Chemistry. In *Organometallic Oxidation Catalysis*, Meyer, F.; Limberg, C., Eds. Springer Berlin Heidelberg: 2007; Vol. 22, pp 79-95.
6. Wade, B.; Knorr, R., *Acrylic Fiber Technology and Applications*. Marcel Dekker, Inc: New York, New York, 1995.
7. Wiles, K. B.; Bhanu, V. A.; Pasquale, A. J.; Long, T. E.; McGrath, J. E., *Journal of Polymer Science, Part A: Polymer Chemistry* 2004, 42, 2994-3001.
8. Robert R. Matzke, J., *Acrylic Fiber Technology and Applications*. Marcel Dekker, Inc.: New York, New York, 1995.
9. Brito Junior, C. A. R.; Pardini, L. C.; Alves, N. P.; Fleming, R. R.; Zavec, I. C. PAN Fibers Obtained by Extrusion Process using Glycerin as Plasticizer http://www.quimlab.com.br/pdf/congresso_carbono_carlos.pdf (accessed April 14,2014).
10. Frushour, B. G., *Acrylic Fiber Technology and Applications*. Marcel Dekker, Inc.: New York, New York, 1995.
11. Smierciak, R. C.; Jr., E. W.; Ball, L. E. Process for making a high nitrile multipolymer prepared from acrylonitrile and olefinically unsaturated monomers. 5,618,901, April 8, 1997.
12. Bhanu, V. A.; Rangarajan, P.; Wiles, K.; Bortner, M.; Sankarpandian, M.; Godshall, D.; Glass, T. E.; Banthia, A. K.; Yang, J.; Wilkes, G.; Baird, D.; McGrath, J. E., *Polymer* 2002, 43, 4841-4850.
13. Moad, G., Radical Polymerization. In *Polymer Science: A Comprehensive Review*, Matyjaszewski, K.; Moller, M., Eds. Elsevier: 2012; Vol. 3, pp 59-118.
14. Odian, G., *Principles of Polymerization*. John Wiley & Sons: 2004.
15. Chiefari, J.; Chong, Y. K.; Ercole, F.; Krstina, J.; Jeffery, J.; Le, T. P. T.; Mayadunne, R. T. A.; Meijs, G. F.; Moad, C. L.; Moad, G.; Rizzardo, E.; Thang, S. H., *Macromolecules* 1998, 31, 5559-5562.
16. Ting, S. R. S.; Davis, T. P.; Zetterlund, P. B., *Macromolecules* 2011, 44, 4187-4193.
17. Barner-Kowollik, C.; Buback, M.; Charleux, B.; Coote, M. L.; Drache, M.; Fukuda, T.; Goto, A.; Klumperman, B.; Lowe, A. B.; McLeary, J. B.; Moad, G.; Monteiro, M. J.; Sanderson, R. D.; Tonge, M. P.; Vana, P., *Journal of Polymer Science Part A: Polymer Chemistry* 2006, 44 (20), 5809-5831.
18. Tang, C.; Kowalewski, T.; Matyjaszewski, K., *Macromolecules* 2003, 36, 8587-8589.
19. Liu, X.-H.; Zhang, G.-B.; Lu, X.-F.; Liu, J.-Y.; Pan, D.; Li, Y.-S., *Journal of Polymer Science Part A: Polymer Chemistry* 2006, 44 (1), 490-498.
20. An, Q.; Qian, J.; Yu, L.; Luo, Y.; Liu, X., *Journal of Polymer Science Part A: Polymer Chemistry* 2005, 43 (9), 1973-1977.
21. Liu, X.-H.; Li, Y.-G.; Lin, Y.; Li, Y.-S., *Journal of Polymer Science Part A: Polymer Chemistry* 2007, 45 (7), 1272-1281.

22. Liu, X.-h.; Zhang, G.-b.; Li, B.-x.; Bai, Y.-g.; Pan, D.; Li, Y.-s., *European Polymer Journal* 2008, 44 (4), 1200-1208.
23. Aqil, A.; Detrembleur, C.; Gilbert, B.; Jerome, R.; Jerome, C., *Chemistry of Materials* 2007, 19, 2150-2154.
24. Carlson, J. S.; Hill, M. R.; Young, T.; Costanzo, P. J., *Polymer Chemistry* 2010, 1 (9), 1423.
25. Chernikova, E. V.; Poteryaeva, Z. A.; Belyaev, S. S.; Sivtsov, E. V., *Russian Journal of Applied Chemistry* 2011, 84 (6), 1031-1039.
26. Chernikova, E. V.; Poteryaeva, Z. A.; Belyaev, S. S.; Nifant'ev, I. E.; Shlyakhtin, A. V.; Kostina, Y. V.; Cherevan, A. S.; Efimov, M. N.; Bondarenko, G. N.; Sivtsov, E. V., *Polymer Science Series B* 2011, 53 (7-8), 391-403.
27. Liu, X.-H.; Zhang, G.-B.; Li, B.-X.; Bai, Y.-G., *Journal of Applied Polymer Science* 2009, 114 (1), 663-670.
28. Wan, L.-S.; Lei, H.; Ding, Y.; Fu, L.; Li, J.; Xu, Z.-K., *Journal of Polymer Science Part A: Polymer Chemistry* 2009, 47, 92-102.
29. Feng, M.; Chen, Y.; Gu, L.; He, N.; Bai, J.; Lin, Y.; Zhan, H., *European Polymer Journal* 2009, 45, 1058-1064.
30. Yue, Z.; Wang, D. X.; Liu, J. Q.; Zhang, J.; Feng, S. Y., *Chinese Chemical Letters* 2012, 23 (8), 989-992.
31. Kim, J. S.; Jeon, H. J.; Lee, K. M.; Im, J. N.; Youk, J. H., *Fibers and Polymers* 2010, 11 (2), 153-157.
32. Qin, J.; Zhang, L.; Jiang, H.; Zhu, J.; Zhang, Z.; Zhang, W.; Zhou, N.; Cheng, Z.; Zhu, X., *Chemistry* 2012, 18 (19), 6015-21.
33. Niu, S.; Zhang, L.; Zhu, J.; Zhang, W.; Cheng, Z.; Zhu, X., *Journal of Polymer Science, Part A: Polymer Chemistry* 2013, 51, 1197-1204.
34. Bashir, Z.; Church, S. P.; Price, D. M., 1993, *Acta Polymer* (44), 211-218.
35. Brandrup, J. I., Edmund H.; Grulke, Eric A.; Abe, Akihiro; Bloch, Daniel R. , II. Polymerization and Depolymerization: Decomposition Rates of Free Radical Initiators. In *Polymer Handbook* [Online] John Wiley & Sons: 1999, 2005.
36. Lutz, J.-F.; Neugebauer, D.; Matyjaszewski, K., *Journal of the American Chemical Society* 2003, 125, 6986-6993.
37. Moad, G.; Rizzardo, E.; Thang, S. H. A Micro Review of Reversible Addition/Fragmentation Chain Transfer (RAFT) Polymerization *Controlled Radical Polymerization Guide: RAFT, ATRP, NMP* [Online], 2012, p. 19-26.
38. Chong, Y. K.; Moad, G.; Rizzardo, E.; Thang, S. H., *Macromolecules* 2007, 40, 4446-4455.
39. Niu, S.; Zhang, L.; Zhu, J.; Zhang, W.; Cheng, Z.; Zhu, X., *Journal of Polymer Science, Part A: Polymer Chemistry* 2012, 51, 1197-1204.
40. Kurata, M.; Tsunashima, Y., Viscosity- Molecular Weight Relationships and Unperturbed Dimensions of Linear Chain Molecules. In *Polymer Handbook*, Brandup, J.; Immergut, E. H.; Grulke, E. A.; Abe, A.; Bloch, D. R., Eds. John Wiley & Sons: 1999; 2005; p 68.
41. Brar, A. S.; Goyal, A. K.; Hooda, S., *Pure Applied Chemistry* 2009, 81 (3), 389-415.
42. Vidotto, G.; Crosato-Arnaldi, A.; Talamini, G., Polymerization of Acrylonitrile in the Presence of Different Solvents. *Die Makromolekulare Chemie* 1969, 122, 91-104.
43. Hiemenz, P.; Lodge, T., *Polymer Chemistry*. CRC Press: Boca Raton, FL, 2007.

44. Andrews, R. J.; Grulke, E. A., Glass Transition Temperatures of Polymers. In *Polymer Handbook*, Brandup, J. I., E. H.; Grulke, E. A.; Abe, A.; Bloch, D. R., Ed. John Wiley & Sons: 1999; 2005; p 253.
45. Andrews, R. J.; Grulke, E. A., Glass Transition Temperature of Polymers. In *Polymer Handbook*, Brandup, J. I., E. H.; Grulke, E. A.; Abe, A.; Bloch, D. R., Ed. John Wiley & Sons: 1999, 2005; p 200.